

2-9-1993

Novel Cylindrical Illuminator Tip for Ultraviolet Light Delivery

Hanqun Shangguan
Portland State University

Follow this and additional works at: https://pdxscholar.library.pdx.edu/open_access_etds



Part of the [Electrical and Electronics Commons](#)

Let us know how access to this document benefits you.

Recommended Citation

Shangguan, Hanqun, "Novel Cylindrical Illuminator Tip for Ultraviolet Light Delivery" (1993). *Dissertations and Theses*. Paper 4647.

<https://doi.org/10.15760/etd.6531>

This Thesis is brought to you for free and open access. It has been accepted for inclusion in Dissertations and Theses by an authorized administrator of PDXScholar. Please contact us if we can make this document more accessible: pdxscholar@pdx.edu.

AN ABSTRACT OF THE THESIS OF Hanqun Shangguan for the Master of Science in Electrical Engineering, presented February 9, 1993.

Title: Novel Cylindrical Illuminator Tip for Ultraviolet Light Delivery

APPROVED BY THE MEMBERS OF THE THESIS COMMITTEE:



Lee W. Casperson, Chairman



Thomas E. Haw



Malgorzata Chrzanowska-Jeske



Bradford R. Crain

The design, processing, and sequential testing of a novel cylindrical diffusing optical fiber tip for ultraviolet light delivery is described. This device has been shown to uniformly (+/- 15%) illuminate angioplasty balloons, 20 mm in length, that are used in an experimental photochemotherapeutic treatment of swine intimal hyperplasia. Our experiments show that uniform diffusing tips of

< 400 micron diameter can be reliably constructed for this and other interstitial applications. Modeling results indicate that this design is scalable to smaller diameters.

The diffusing tips are made by stripping the protective buffer and etching away the cladding over a length of 20 mm from the fiber tip and replacing it with a thin layer of optical epoxy mixed with Al_2O_3 powder. To improve the uniformity and ease of fabrication, we have evaluated a new device configuration where the tip is etched into a modified conical shape, and the distal end face is polished and then coated with an optically opaque epoxy. This is shown to uniformly scatter $\sim 70\%$ of the light launched into the fiber without forward transmission. To our knowledge, we are the first to use this device configuration, and we have achieved a uniform cylindrical pattern of laser energy with uniformity $< \pm 15\%$ of the average value.

A simple computational model suitable for the interpretation of laser energy irradiance along the bare core surface of multimode optical fiber tips is proposed and experimentally verified. The model used is based on geometrical optics and Gaussian approximation. Good agreement is obtained between the calculation and experiment.

We have measured the optical properties of the tips through all the sequences of the fabrication. The performances of the diffusing tips for illuminating angioplasty balloons are then evaluated by Ultraviolet Light at 365 nm. A Ti:Sapphire Ring Laser System with a doubling crystal pumped by an argon ion laser is used to generate the wavelength in this study.

NOVEL CYLINDRICAL ILLUMINATOR TIP FOR ULTRAVIOLET
LIGHT DELIVERY

by

HANQUN SHANGGUAN

A thesis submitted in partial fulfillment of
requirements for the degree of

MASTER OF SCIENCE
in
ELECTRICAL ENGINEERING

Portland State University
1993

TO THE OFFICE OF GRADUATE STUDIES:

The members of the Committee approve the thesis of Hanqun Shangguan presented February 9, 1993.



Lee W. Casperson, Chairman



Thomas E. Haw



Malgorzata Chrzanowska-Jeske



Bradford R. Crain

APPROVED:



Rolf Schaumann, Chairman, Department of Electrical Engineering



Roy W. Koch, Vice Provost for Graduate Studies and Research

ACKNOWLEDGMENTS

This study has been supported by the encouragement of many people. First, I would like to express heartfelt appreciation to my Academic Adviser, Dr. Lee W. Casperson, for all the guidance, help, and encouragement he gave me throughout my study for MSEE degree in the Department of Electrical Engineering, Portland State University.

I would also like to thank Mr. Thomas E. Haw, the technical director of Cardiovascular Laser Research Center, St. Vincent Hospital & Medical Center, for his kind instruction, and his intellectual stimuli throughout this research program, which have greatly influenced my perspectives. His expertise and total involvement in this program made this thesis possible.

I extend appreciation also to Dr. Kenton W. Gregory, MD, the director of the Cardiovascular Laser Research Center, who has provided me the excellent opportunity to study and work at the center. I would not have been able to achieve so much on this research program without his great help.

Thanks also to the other members of the "Gregory Team", Dr. Ned Chastaney, MD, Micki Spent, Lisa Buckley, Karen Elings, and Deb Tuke-Bahlman, RN, for their hospitality, encouragement, and the pleasure we shared at the center. I am especially thankful to Dr. Scott Prah, for his thoughtful ideas and his time.

Thanks to Dr. Malgorzata Chrzanowska-Jeske, and Dr. Bradford R. Crain, for providing valuable comments on my thesis.

I would like to thank my mother Dr. Jingyun Chen, MD, my father Prof. Zongnan Xia, MD, my mother-in-law Ms. Pingxia Ni, my father-in-law Mr. Yingen Zhu, and my brother Dr. Xiaochu Shangguan, MD, for supporting me spiritually and financially for years. Thanks also to my grandfather Mr. Ta Tseng for his initial financial support for my attendance at Portland State University. It would have been very hard or impossible for me to present this thesis without his generosity.

Finally, I wish to dedicate this thesis to my wife Dr. Zhenghong Zhu, MD, and daughter Xingzi, whose patience, understanding, and confidence in me made this all possible.

TABLE OF CONTENTS

	PAGE
ACKNOWLEDGMENTS	iii
LIST OF TABLES	vii
LIST OF FIGURES	viii
CHAPTER	
I INTRODUCTION	1
II DEVICE DESCRIPTION	5
III DESIGN CONSIDERATIONS	8
VI FABRICATION TECHNIQUE	15
Geometric Preparation	15
Coating Technique	21
V EXPERIMENTAL RESULTS	24
Light Coupling to the Diffusing Tip	24
Effect of Scattering Material on the Light Distribution	26
Effect of Light Coupling on the Light Distribution	27
Reproducibility of the Fabrication Technique	31
Results for the Device to Illuminate an Angioplasty	
Balloon	32
VI DISCUSSION	35
VII CONCLUSION	38
REFERENCES	39

APPENDIXES

A	CALCULATION OF LIGHT DISTRIBUTION ON THE BARE CORE SURFACE OF THE FIBER TIP	43
B	DERIVATION OF Eq.(A2)	53

LIST OF TABLES

TABLE		PAGE
I	The Geometric Parameters of a Tip	19
II	Measured Optical Power along an Angioplasty Balloon	34

LIST OF FIGURES

FIGURE		PAGE
1.	How the laser energy is delivered to turn on the drug at the site of illumination inside artery	2
2.	A diffusing tip (at bottom) and an angioplasty balloon with the diffusing tip (on top)	2
3.	Schematic diagram of illuminator tip	6
4.	Schematic diagram of multipurpose guiding catheter	7
5.	Schematic diagram of three different tip shapes	9
6.	Schematic diagram in cross section of a tapered cylindrical optical fiber with taper angle equal to α	10
7.	Schematic of etching apparatus	16
8,	Scanning micrograph of bare core surface of a fiber tip after etching with magnification 10,000X	18
9.	Block diagram of geometry preparation procedure	20
10.	Block diagram of coating procedure	23
11.	Experimental setup for convergence angle measurement	25
12.	Experimental setup for measuring the effect of scattering material on the light distribution	26
13.	Measured irradiance at one tip: (a) without powder; (b) powder concentration = 285 mg/ml; (c) powder concentration = 570 mg/ml	28
14.	Arrangement for measuring the effect of light coupling on the light distribution	29
15.	Measured irradiance at a distance of 1.75 mm from the fiber axis for one fiber at two different convergence angles θ , normalized to the maximum value, for (a) $\theta = 5^\circ$; (b) $\theta = 8^\circ$	30

FIGURE		PAGE
16	Measurement apparatus for the reproducibility of the tips	31
17.	Measured irradiance showing the reproducibility of the fabrication technique	32
18.	Assembly for the device to illuminate an angioplasty balloon	33
19.	Schematic diagram of Hockey Stick Catheter	37

CHAPTER I

INTRODUCTION

Photochemotherapeutic treatment of intimal hyperplasia may reduce the healing response to balloon injury or restenosis¹⁻³. It has potential advantages over surgery, balloon angioplasty, and other forms of vascular intervention. A patient can take a drug in an inert form that has no side effects. Once the drug is in the body, nearly uniform cylindrical irradiation of laser energy emitted from an angioplasty balloon can "turn on" the drug efficiently, creating a therapeutic photochemical reaction only at the site of illumination, thus potentially decreasing the high rate of restenosis that occurs with balloon angioplasty (cf. Figure 1). During the treatment, laser energy is usually delivered circumferentially by an optical fiber that terminates in a central diffusing tip within the inner lumen of an angioplasty balloon. A limiting problem in achievement of a uniform cylindrical pattern of laser energy is the development of a miniature diffusing tip at the distal end of the optical fiber. Figure 2 shows a diffusing tip (at bottom) and an angioplasty balloon with a diffusing tip (on top) illuminated with a He-Ne laser.

Currently the typical optical fiber diffusing tips that may be used for Photodynamic Therapy (PDT) are made by removing the cladding over a desired length from the fiber tip and replacing it with a thin layer of optical scattering material⁴⁻⁶ or attaching the distal end of the fiber to a diffuser⁷⁻¹¹. Both devices provide a nearly uniform cylindrical pattern of irradiation. The best uniformity

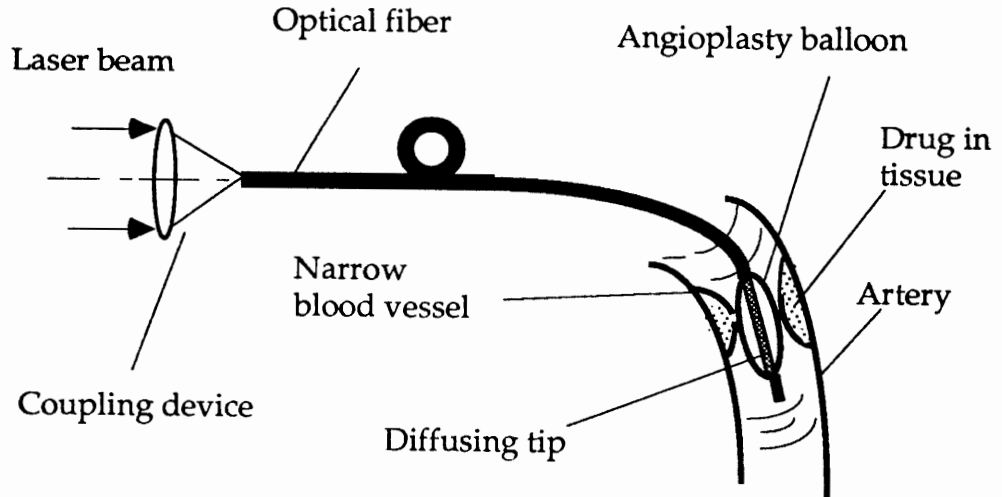


Figure 1. How the laser energy is delivered to turn on the drug at the site of illumination inside artery.

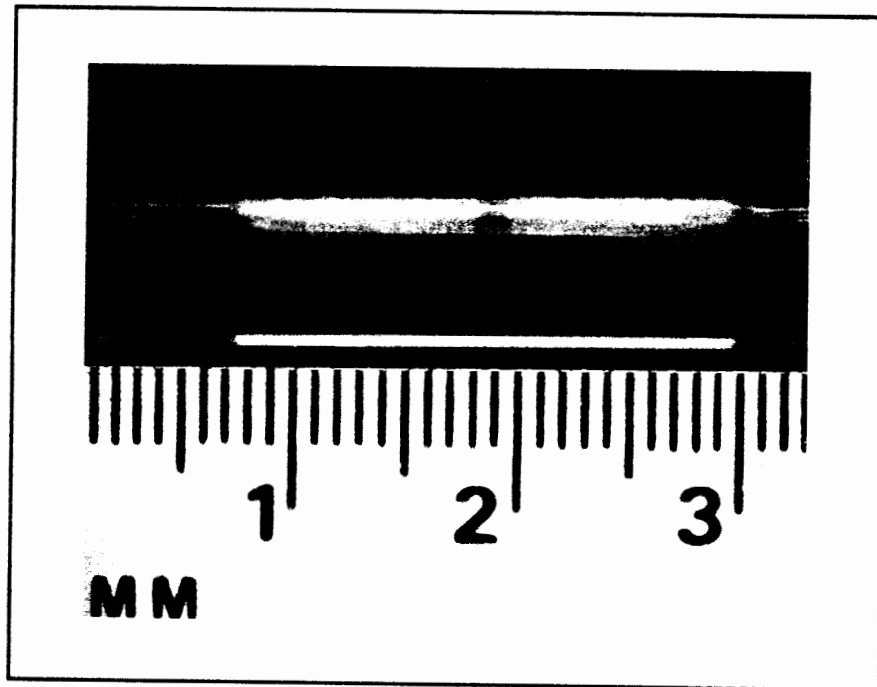


Figure 2. A diffusing tip (at bottom) and an angioplasty balloon with the diffusing tip (on top).

of illumination over a length of 20 mm is about 40% of the average value. Unfortunately, the device configurations are either complex to fabricate or are limited by the angioplasty balloon geometry to smaller diameters.

The objective of the present study is to develop a simple and useful method for the design and fabrication of similar optical scattering devices for PDT. In this paper we report on the fabrication and measurement of a novel cylindrical illuminator tip for UV light delivery primarily designed for use in an experimental photochemotherapeutic treatment of swine intimal hyperplasia. This illuminator can also be utilized in interstitial applications where a miniature (<0.018" diameter) illuminator is required. The diffusing tips are made by stripping the protective buffer and etching away the cladding over a length of 20 mm, and replacing it with a thin layer of optical epoxy mixed with Al_2O_3 powder. To improve the uniformity and ease of fabrication, we have evaluated a new device configuration where the tip is etched into a modified conical shape, and the distal end face is polished and then coated with an optically opaque epoxy. This is shown to uniformly scatter ~70% of the light launched into the fiber without forward transmission. To our knowledge, we are the first to use this device configuration, and we have achieved a uniform cylindrical pattern of laser energy with uniformity $< \pm 15\%$ of the average value.

A part of this study was presented (oral presentation) at the International Symposium on Laser, Fiber, and Clinical Imaging in Medicine, on Feb. 17, 1993, in Los Angeles, CA, and it will be published in SPIE proceedings Vol. 1878, 1878-30, 1993. This device and the fabrication methods of making same have been submitted in a United States patent application.

Fibers with modified tip and powder admixtures are tested. Various convergence angles are used for the He-Ne laser beam coupled into the fiber in these tests. We find that all of these parameters have a significant effect on the optical performance of the fiber diffusing tip. The performances of the diffusing tips to illuminate angioplasty balloons are then evaluated by ultraviolet light at 365 nm. A Ti:Sapphire Ring Laser System with a doubling crystal, pumped by an argon ion laser, is used to generate the wavelength in this study.

The device description including the principle of operation, device requirements, etc., is described in Chapter II. In Chapter III, we present the qualitative analyses of the device parameters which affect the light distribution at the diffusing tip and some words about quantitative analyses. The detailed fabrication techniques for the diffusing tip are described in Chapter IV. Chapter V includes the experimental setup and observed results. A discussion of the experimental results, and the effects of device parameters on the light distribution is included in Chapter VI. Our study concludes in Chapter VII. A basic computational model for calculating the light distribution along the bare core surface of a fiber tip is described in the Appendix A. The Appendix B contains a brief derivation showing how a Gaussian beam given as a function of radial position can be transferred into a function of angular position.

CHAPTER II

DEVICE DESCRIPTION

A schematic diagram of the illuminator tip is shown in Figure 3. Being coupled into the fiber at an angle that is equal to or larger than the critical angle, laser beam is transmitted, unattenuated, within a lossless fiber¹². When the laser radiation propagates into the diffusing tip section, the total internal reflection properties of the fiber have been lost and an anti-guiding situation occurs due to the higher index of the coating [optical epoxy ($n_D = 1.56$) and powder ($n_D = 1.65$)]. Light propagating in the lower refractive index core ($n_D = 1.46$) is redistributed at each Fresnel reflection between the core and the scattering layer. Depending on the angle of incidence, some of the light is refracted into the scattering layer, and a fraction is reflected to the other side of the wall and then redistributed again at the core-layer interface. In this manner, each original ray generates an increasing number of subrays of ever-decreasing amplitude as it propagates along the diffusing tip. Therefore, the radiation is sequentially being refracted into the scattering layer and then scattered out of the fiber structure. The anti-guiding configuration significantly redistributes the input radiation along the etched length of the tip.

For the intended use, the diffusing tip is assembled within an angioplasty balloon, 3.5 mm \times 20 mm (MansfieldTM, Boston Scientific Co., Watertown, MA02172), and produces a 20 mm long cylindrical irradiance pattern of laser

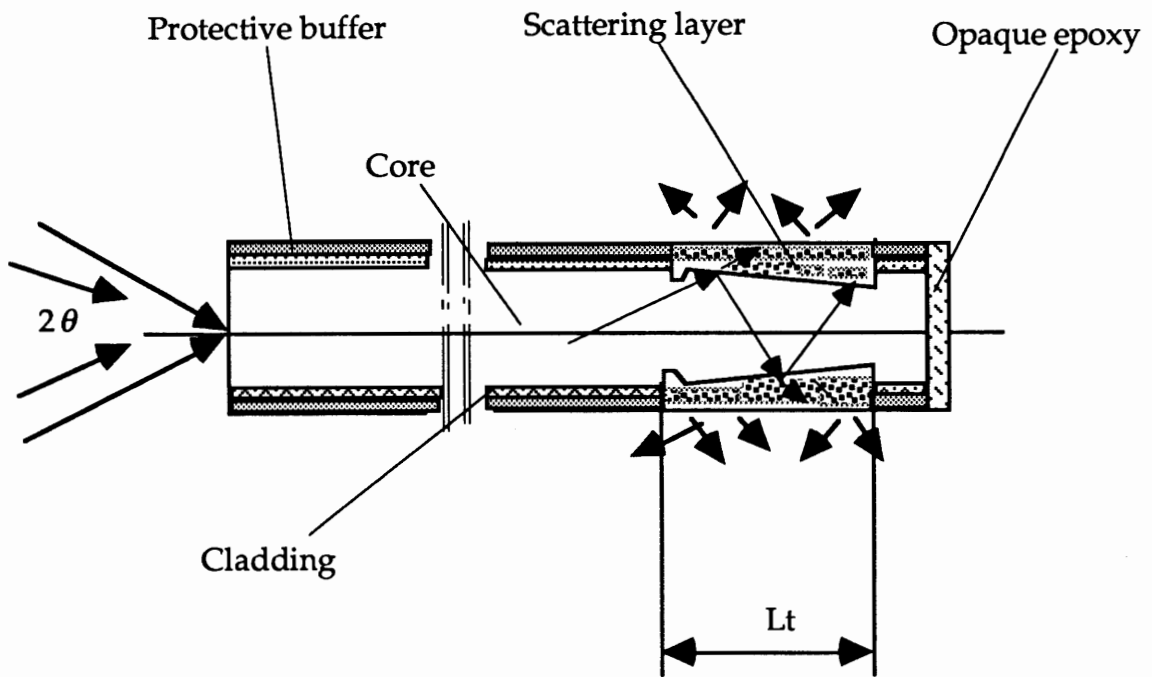


Figure 3. Schematic diagram of illuminator tip.

energy. The balloon is guided by a 7F multipurpose catheter (Super.7TM, USCI Division CR. Bard, Inc., Billerica, MA01821); shown in Figure 4. The requirements for the illuminator tip are as follows:

- (1) Optical performance: The tip should produce uniform irradiance at a radial distance of ~ 1.75 mm from the fiber axis. The magnitude of the radiance of the tip should, therefore, be roughly constant along the length of the tip and rotationally symmetric. Furthermore, it is desirable that the proximal end of the balloon receives minimal or no direct laser exposure.

- (2) Mechanical performance: The diffusing tip should be small in size (the overall diameter is less than $365\ \mu\text{m}$) to be easily introduced into the balloon and provide reasonable safety against fracture.

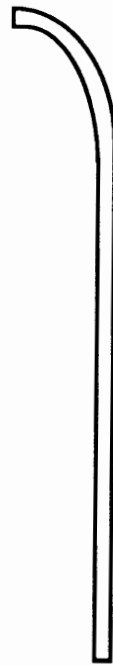


Figure 4. Schematic diagram of multipurpose guiding catheter.

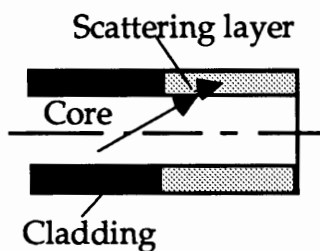
CHAPTER III

DESIGN CONSIDERATIONS

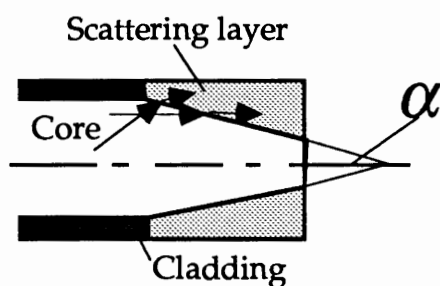
The optical behavior of the diffusing tip depends on the geometry of the tip, the angular distribution of the light input to the diffusing tip (convergence angle of the input laser beam), the refractive index of the core, the refractive index of the scattering layer, and the scattering powder concentration. The qualitative analyses for these parameters are described below.

Figure 5 shows three tips with different geometries. For a cylindrical shape, only the rays at angles with respect to the fiber axis can be refracted from the core [see Figure 5 (a)]. For a conical shape, besides the rays at angles with respect to the fiber axis, some of the rays parallel to the axis can also be refracted from the core [see Figure 5 (b)]. For a modified shape (bi-tapered shape) not only can both rays be refracted from the core, but also more light can be coupled out of the core at the beginning of the tip (In practice, the light power at the first 1~2 mm of a cylindrical shape is lower than the peak value) [see Figure 5 (c)]. The amount of light refracted into the scattering layer also depends on the incident angle at the interface of core-scattering layer¹³. With the incident angle reduced, more light is refracted from the core. For a cylindrical tip, the incident angles of the rays do not change after several reflections. But as a ray is internally reflected in the tapered zone, the incident angle θ_i between the ray and the normal to the core-layer interface will be decreased by the amount α after each reflection (see Figure 6). Therefore, more light leaks out from the taper

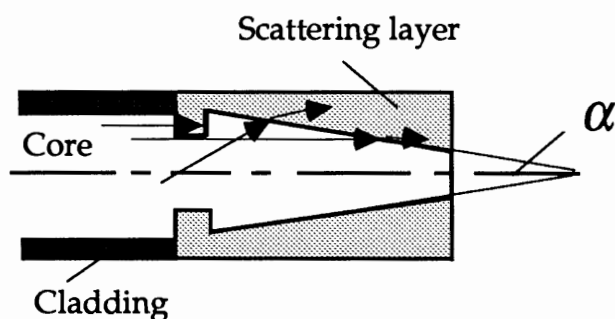
than that for the cylinder. It is obvious that the modified geometry is advantageous to make more light transmitted into scattering layer and then scattered out of the fiber structure than the others.



(a) Cylindrical shape



(b) Conical shape



(c) Modified shape

Figure 5. Schematic diagram of three different tip shapes.

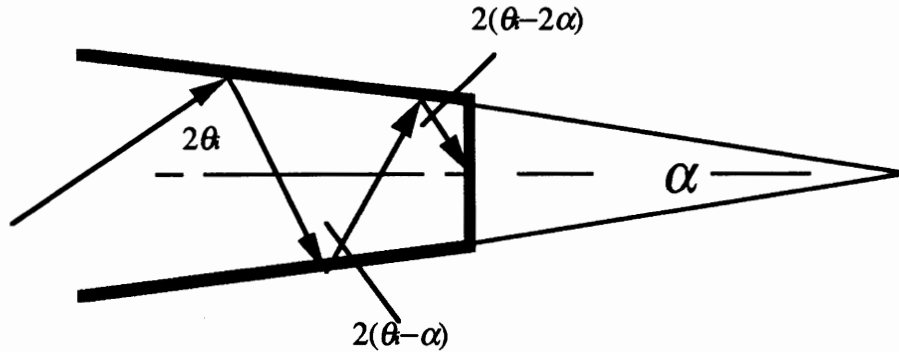


Figure 6. Schematic diagram in cross section of a tapered cylindrical optical fiber with taper angle equal to α .

Fiber optical delivery of laser light is associated with Gaussian beam optics¹⁴. The irradiance distribution of the laser beam emitted from a multimode fiber is usually assumed to have a Gaussian angular distribution¹⁵. Because this Gaussian distribution is related to which fiber modes are excited, considerable variation in displacement of the irradiance peak from the diffusing tip can be achieved by varying the angle of optical coupling into the fiber, i.e., convergence angle. Small convergence angles will excite primarily low-order modes and move the irradiance peak towards the distal end of the tip, while larger convergence angles can excite both low and high-order fiber modes and move the irradiance peak toward the beginning of the tip⁶.

According to Eq.(43) of Ref. 13, the reflectance can be written as

$$R(\beta) = \frac{1}{2} \left[\frac{\tan^2(\beta - \beta')}{\tan^2(\beta + \beta')} + \frac{\sin^2(\beta - \beta')}{\sin^2(\beta + \beta')} \right]$$

where β and β' are the incident angle and refracted angle on the interface of the core-scattering layer respectively.

According to the paraxial approximation (i.e., $n_{core} \cdot \beta = n_{layer} \cdot \beta'$), the reflectance can be replaced by:

$$R(\beta) = \frac{1}{2} \left[\frac{\tan^2(1 - \frac{n_{core}}{n_{layer}})\beta}{\tan^2(1 + \frac{n_{core}}{n_{layer}})\beta} + \frac{\sin^2(1 - \frac{n_{core}}{n_{layer}})\beta}{\sin^2(1 + \frac{n_{core}}{n_{layer}})\beta} \right]$$

where n_{core} , n_{layer} are the refractive index of the core and that of the scattering layer respectively.

From the above equation, it is clear that the reflectance will increase with increasing the refractive index of the scattering layer. Therefore, more light will be reflected toward the distal end of the tip.

The effect of powder concentration is very complex. Usually, with increasing concentration, the scattering coefficient of the scattering layer will increase, and the light will be scattered more times. This may or not lead to greater uniformity of irradiance at the tip depending on the intrinsic absorption of the optical epoxy and powder, and other lossy elements in the fiber tip. The validity of this argument is not questionable when the particles of the powder are widely separated, but doubts arise when the separations are less than or comparable to the wavelength of the light. For a cylindrical optical fiber diffusing tip, the irradiance dependence on the powder concentration is similar to that of the convergence angles⁶, i.e., with increasing powder concentration, the irradiance peak value will move toward the beginning of the tip.

The quantitative analyses of these parameters are not easy. Normally, its solution requires simplifying assumptions and the use of numerical methods. However, almost all of papers related to the fiber optical delivery were either on laser power transmission through optical fiber¹⁶⁻²² or on laser beam profiles and spatial irradiance distributions of the modified bare fiber tips used in laser angioplasty and laser surgery²³⁻³⁰. Up to now, to our knowledge, very few papers^{6,31} have been published on calculations of light distribution at similar optical fiber diffusing tips.

Hasselgren et. al⁶ reported a computer simulation program to simulate the light distribution at a diffusive tip. The program uses rays, a rotationally symmetric bundle of which is assumed to be launched into the fiber, starting on the fiber axis. The ray amplitudes have a Gaussian angular distribution. This approximates a Gaussian laser beam, focused normally onto the center of the input end surface of the fiber. The program traces the various rays as they propagate along the fiber into the diffusive fiber end section. At each Fresnel reflection between the core and the diffusive cladding, a ray is split in two. In this way, each original ray generates an increasing number of subrays with decreasing amplitude as it propagates along the diffusive fiber. The program treats the amplitude of a ray decay inside scattering layer as an exponential function. This program may be useful in design of diffusive fiber tip, but the details of the formulas were not given.

Pan et. al³¹ reported a model to calculate the light distribution from an optical fiber diffuser tip. In their work, the light intensity distribution at near field, i.e., the radial distance from the fiber axis is equal to or less than the diameter of the tip, can be written as

$$I_n = I_n(0) \cdot \exp(-\alpha x)$$

where x is the longitudinal distance along the fiber axis and varies from 0 to the maximum length of the fiber diffuser, α is a coefficient which is a function of the geometrical and material parameters of the diffuser, and can be expressed as

$$\alpha = \alpha(n_c, n_e, n_p, d, t, \theta_i)$$

where n_c, n_e, n_p are the indices of refraction of core, epoxy, and scattering powder respectively, d is the fiber diameter, t is the thickness of the scattering layer, and θ_i is the convergence angle of the input laser beam.

On the basis of the light distribution in the near field, the light distribution in the far field, i.e., the radial distance from the fiber axis is larger than the diameter of the tip, can be easily obtained by modifying one in the near field with cosine law of illumination and the inverse square law. The light intensity at any point in the space around a fiber optical diffuser is given by

$$I_f = \int \left\{ I_n(0) \cdot \exp(-\alpha x) \cdot \frac{D^2}{[D^2 + (a-x)^2]^2} \right\} \cdot dx$$

where D is the distance from a point in space to the fiber axis, a is the longitudinal distance from 0 to the point in space.

Unfortunately, the calculation of the key factor α , which is assumed to be a known function in the paper, is not given.

Although many factors affect the distribution of laser irradiance on the illuminator tip surface such as the geometry of the tip, fiber numerical aperture, convergence angle of the input laser beam, tapered tip length, and scattering powder concentration, a successful understanding of laser energy radiation along the bare core surface of an optical fiber tip is very important for the design and fabrication of optical fiber diffusing tip. To try to avoid the difficulty of calculating the light distribution at the diffusing tip, we have developed a simple computational model to calculate the light distribution along the bare core surface of an optical fiber tip for fabrication of the diffusing tip. The details of the computational model are given in the Appendix A.

On the basis of the effects of these parameters on the light distribution at the tip, a uniform cylindrical irradiance pattern of laser energy can be obtained through optimization of the parameters. For example, a good uniformity of illumination can be achieved by varying the concentration of the scattering powder along the length of the diffusing tip¹⁰ or increasing the scattering layer thickness along the fiber end⁶. The method we have chosen in this study is to modify the geometry of the tip on the basis of a known convergence angle of input beam.

Approximately 8 mm of the buffer and cladding are left at distal end for ease of tip assembly inside an angioplasty balloon and for enhancement of the bending strength. The optically opaque epoxy is coated on the distal face to stop the transmitted light power in the forward direction so as to ensure that the proximal end of the balloon receives minimal or no direct laser exposure.

CHAPTER IV

FABRICATION TECHNIQUE

A flexible, optical fiber with 300 μm core diameter and 0.22 numerical aperture (Polymicro Technologies, Phoenix, AZ) is used in this study. The fiber is a step-index multimode fiber with a synthetic fused silica core, silica cladding, and protective polyimide buffer. The detailed fabricating procedure for the illuminator tip is described as follows.

GEOMETRY PREPARATION

After a piece of silica fiber has been cut (2 m-2.5 m), one of the distal faces is wet-polished flat as the input end of the fiber using standard fiber polishing techniques. At its other end, the protective buffer is thermally removed with a pyrolytic stripper over 20 mm, with 10 mm left from the distal end of the fiber (see Figure 3). The tip is then fabricated into a modified shape by a chemical etching technique. The chemical used is Hydrofluoric Acid (48%). The length of time that the tip is exposed to the acid determines the tapered shape. The polyimide buffer protects the fiber from etching. To form the modified tip, two methods are studied:

- (1) After removing the protective buffer, the optical fiber is supported in a vertical position by attaching it on a vertical translator (Line Tool Co.,

AllenTown, PA) and then dipped into Hydrofluoric Acid gradually (the increment is ~ 0.4 mm). The apparatus for etching is shown in Figure 7.

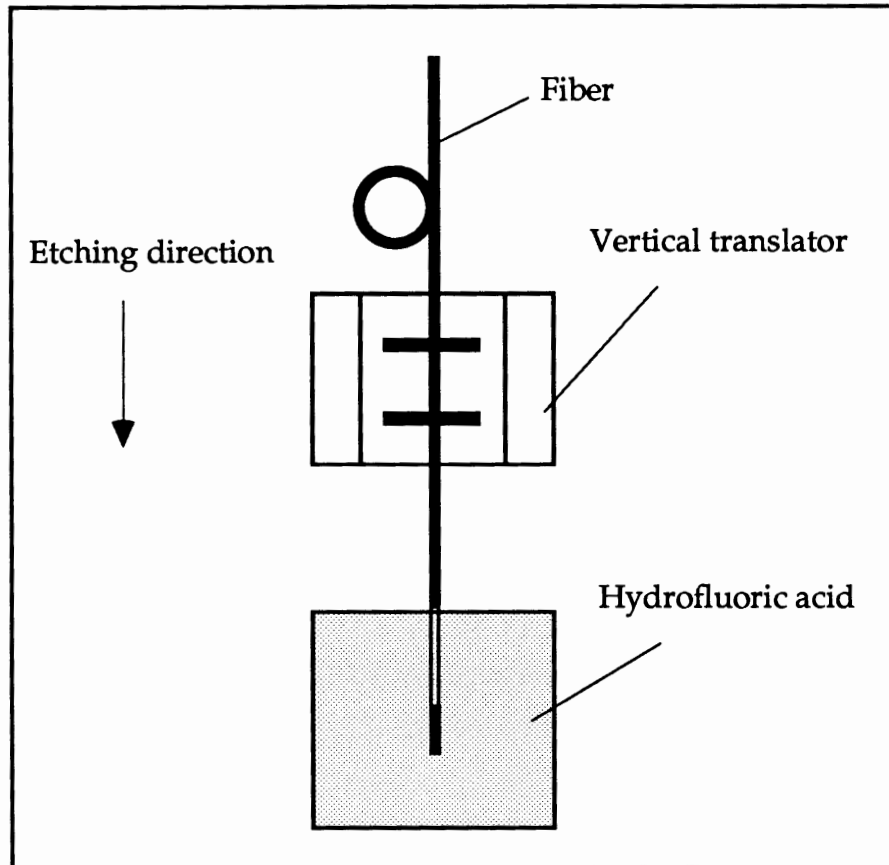


Figure 7. Schematic of etching apparatus.

The etching time for each increment is about 20 seconds. During this period, the cladding is usually etched away. The optical fiber is examined under an optical microscope after the buffer and cladding are removed to ensure that the geometry of the fiber end is correct with a suitable etching rate. Although the etching rate is usually $4 \mu\text{m}$ in diameter per minute, since the etching rate is not linear, it has to be determined experimentally based on the etching conditions such as quality of the fiber, chemical bath, etc.. For example, in

practice, it takes 4 minutes and 22 seconds to etch away 20 μm in diameter, the ratio is about 4.58 μm in diameter per minute, but it takes 18 minutes to etch away 50 μm in diameter, the ratio is about 2.8 μm in diameter per minute. The modified tip can be obtained by partially covering the area where the irradiance with peak value is located with some Hydrofluoric Acid resistant materials such as Polyimide Tubing (Polymicro Technologies, Phoenix, AZ), photoresist (Shipley photoresist 1350J)²³, etc.. The area can be determined by measuring or calculating the light distribution at the tip (cf. Appendix A). The uncovered portion at the fiber end together with the covered portion is then dipped into the acid to form the modified shape. In our case, it takes three and a half minutes for this step. The resulting bi-tapered tip is dipped into an epoxy/powder mixture (the weight ratio of EPO-TEK[®] 301-2 to Al_2O_3 is 10 to 3, i.e., the powder concentration is 285 mg/ml) and then the irradiance distribution at the tip is measured with a known convergence angle, in our case, $\theta = 5^\circ$. The measurement technique will be described in Chapter V. If the irradiance distribution is not uniform, the mixture can be cleaned away easily with Acetone, and then the etching can be repeated until a uniform irradiance is obtained.

(2) A similar procedure to that described above is utilized for the fabrication of a modified tip, with the exception that the buffer and cladding are removed first and then the fiber is fabricated into bi-tapered shape.

The bare core surface of a fiber tip is inspected with a Scanning Electron Microscope after etch (cf. Figure 8). The scanning micrograph shows that the bare core surface is smoothly rough. The geometric parameters of a bare tip are shown in Table I. A summary of Geometry Preparation Procedure is illustrated in Figure 9.

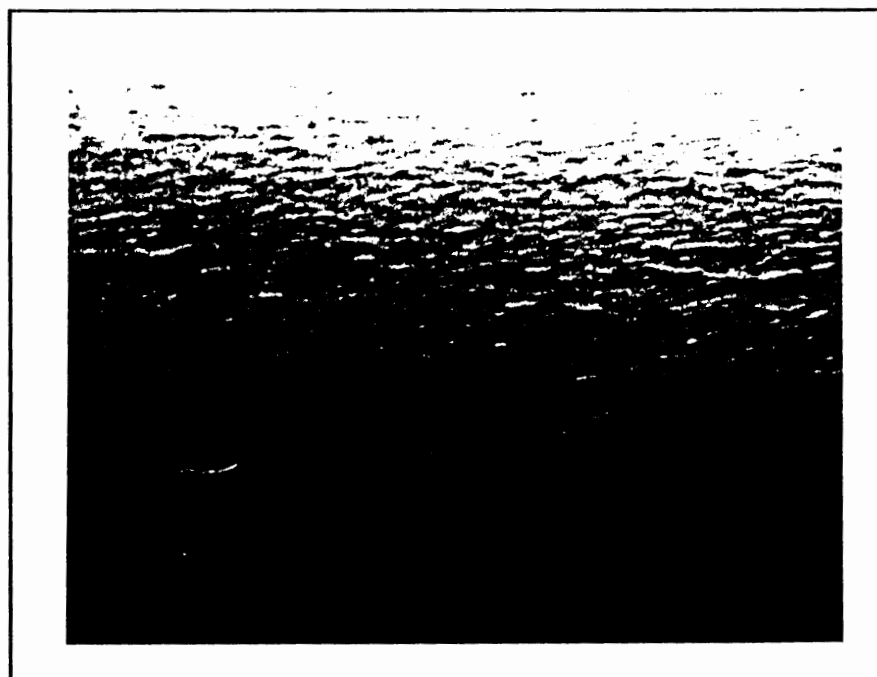


Figure 8. Scanning micrograph of bare core surface of a fiber tip after etching with magnification 10,000X.

There are two points we should mention here: (1) it is essential to remove cleanly all cladding material so that the irradiance peak position can be covered correctly; (2) excessive handling the bare tip should be avoided. Otherwise, the tip may become brittle. In practice, besides the methods mentioned above, we have applied the UV light curing technique to cover the irradiance peak position. The procedure is described below.

During covering of irradiance peak position, the area is covered with UV epoxy (LITETAK 376, Loctite Co., Newington, CT0611) mixed with Al_2O_3 powder (the weight ratio of UV epoxy to Al_2O_3 powder is 10 to 3) and then the mixture is cured with UV light for about 5 seconds. After that the tip is dipped into

TABLE I
THE GEOMETRIC PARAMETERS OF A TIP

Tip Length	Z (mm)	Core Diameter d (μm)
	0	299
	0.5	297
	1	295
	2	295
	3	299
	4	298
	5	294
	6	291
	7	288
	8	285
	9	282
	10	279
	11	277
	12	274
	13	271
	14	268
	15	265
	16	262
	17	259
	18	256
	19	253
	20	250

Note: Those data are obtained using an optical microscope with 10x magnification, so the data only show the rough geometry.

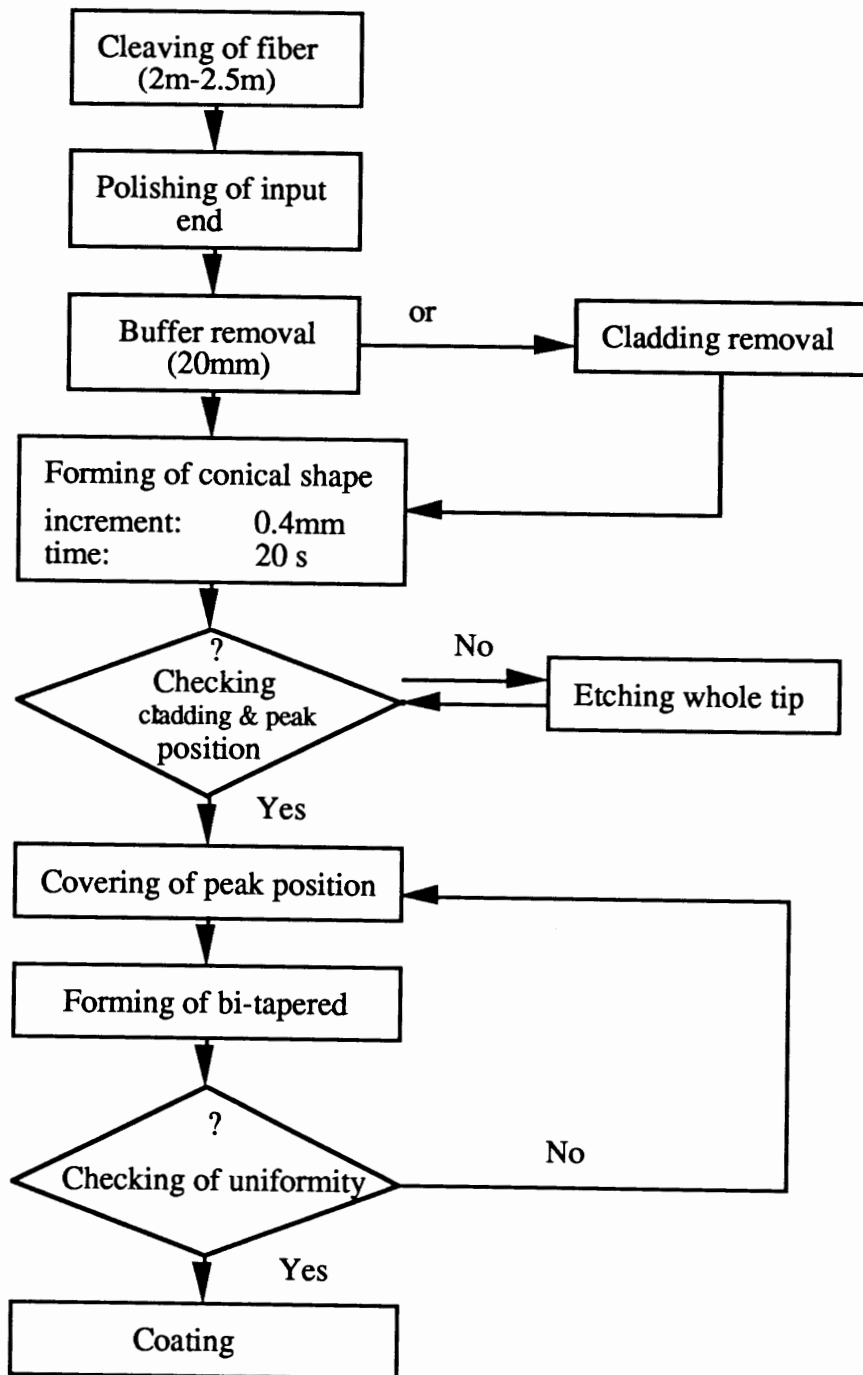


Figure 9. Block diagram of geometry preparation procedure.

Hydrofluoric Acid for 3.5 minutes. Then the tip is washed with water, and the cured mixture can be removed mechanically, if not, the Chlorinated Hydrocarbon/Equipment Flushing Solvent (Loctite Co., Newington, CT0611) can be used to easily solve the cured mixture. It takes ~ 1.5 minutes to solve the cured mixture on the tip. Since the cured mixture on the tip is not an excellent Hydrofluoric Acid resist, it will be dissolved partially or totally after about 4 minutes in the acid. Therefore, it is not suitable to protect the tip from etching if the length of etching time is longer than that. However, just following the simple procedure mentioned above, the fabricated tip can produce a cylindrical irradiance pattern of laser energy with uniformity $< \pm 25\%$ of the average value.

COATING TECHNIQUE

The fiber tip is carefully cleaned with Acetone before it is coated. The clear, two component optical epoxy (EPO-TEK[®] 301-2) is prepared by thoroughly mixing it with a carefully weighed amount of Al_2O_3 powder as the coating material. The weight ratio of the optical epoxy to powder Al_2O_3 is 10 to 3, i.e., the powder concentration is 285 mg/ml. The powder Al_2O_3 used is commercial grade (Linde A, the typical grain size being ~ 0.3 μm). A piece of Teflon tube (28GA, SMALL PARTS INC., Miami, FL33238) is cut (35 mm in length), and then the tip is inserted into the tube. The tube is heated using a hot-air gun or a hotplate until it becomes straight. Coating the tip with the coating material is simultaneous with moving the tube backwards and forwards along the tip, so that the space between the inside wall of the tube and the tip is filled with the coating material without any air bubbles. Small air bubbles are removed by warming the epoxy/ Al_2O_3 mixture with a hotplate or a hot-air gun. (This procedure should be done for both of a container with coating material and

the coating tip simultaneously.) Then the tip is allowed to dry in vertical position under a warm situation (about 75F⁰). After the drying, the Teflon tube can be removed thermally. During removal of the tube, we put a metal block on a hotplate and warm it to above 212F⁰, and we then put the tube in contact with the metal block and remove the tube with a pair of tweezers as soon as possible. Otherwise, the heating can damage the coating material. After the drying, there are usually some small holes on the scattering layer due to the different tension in the layer surface during drying. The holes can be fixed easily with the epoxy/ Al₂O₃ mixture. Finally, the distal face at the end of the tip is cleaved (8 mm left) and polished, and then coated with an optically opaque epoxy (EPO-TEK[®] 320, whose transmission is less than 0.0001% at 300 nm-1 micron). A summary of the Coating Procedure is illustrated in Figure 10.

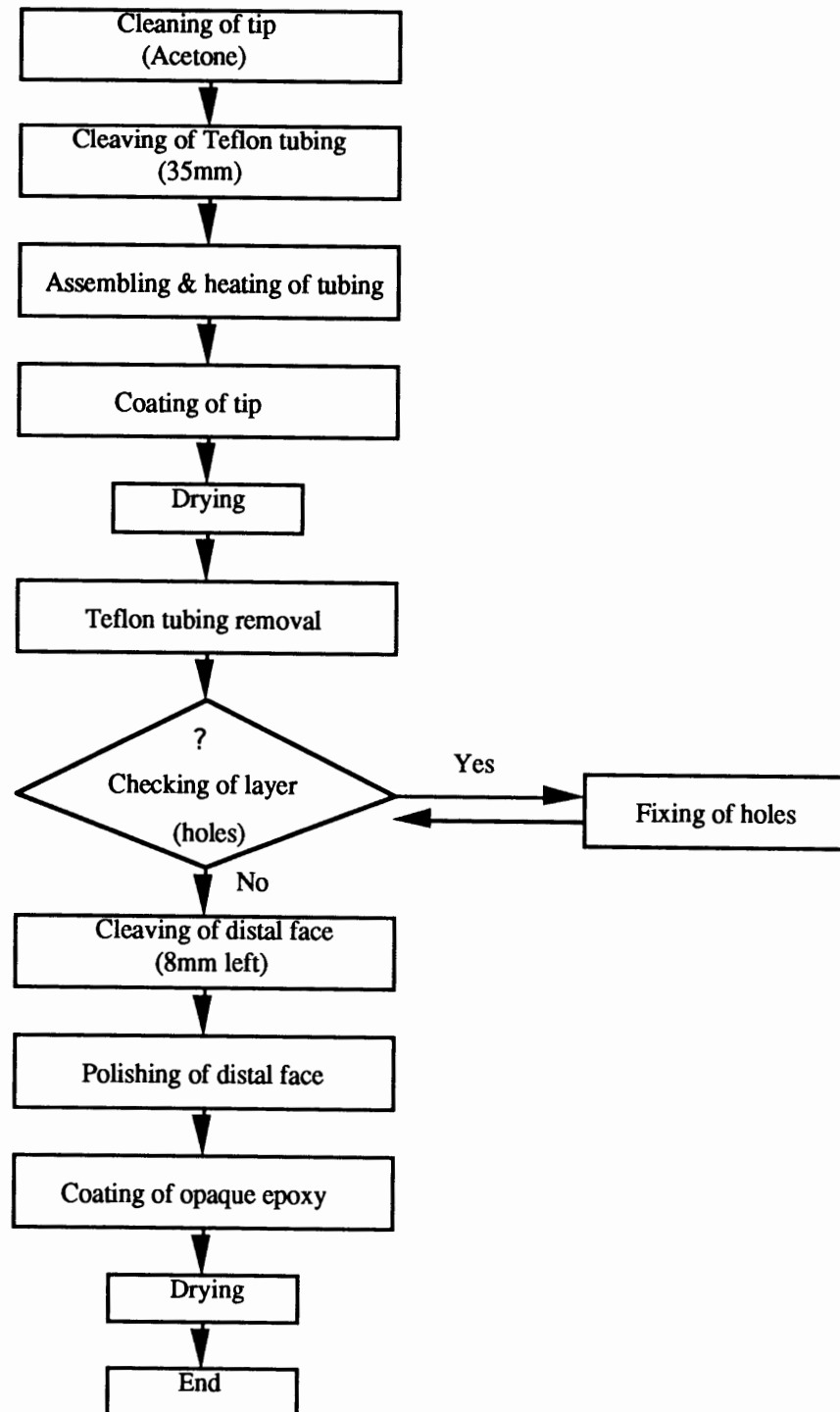


Figure 10. Block diagram of coating procedure.

CHAPTER V

EXPERIMENTAL RESULTS

LIGHT COUPLING TO THE DIFFUSING TIP

The convergence angle of the input beam refers to the half angle θ which characterizes the axial cone in a uniform beam of light converging on to the fiber end. When one launches light at a smaller angle than the acceptance angle of the fiber, at least over short lengths, the output beam is narrower. It is this narrow distribution of light that is input to the diffuser element. There are two techniques³² for directly measuring the relative ability of fibers to accept power launched from different cone angles:

1. The fiber acceptance-angle technique, which measures the relative power launched as a function of launch cone angle
2. The fiber radiation-angle technique, which measures the relative power radiated as a function of output cone angle.

In our case, the second technique is used for directly measuring the output beam θ_o . Since the output beam is related to the input one, e.g., the convergence angle of the input beam is equal to the output angle, at least for a straight fiber¹², in this way, we can obtain the convergence angle of the input beam. A common launch-optics arrangement is used; see Figure 11. The both distal faces of the tested fiber, a silica optical fiber with 400 μm core diameter (Polymicro

Technologies, Phonix, AZ), are wet-polished flat. Optimum coupling is achieved by maximizing the output optical power. Efficiency approximately ~ 80% is observed. The convergence angles of the input beam at the entrance face of the tested fiber are easily obtained through adjusting the optical system. The angle of output beam θ_o is given by

$$\theta_o = \tan^{-1} \frac{D}{2L}$$

as shown in Figure 11. D is the beam spot size on the diffusive plane (a piece of white paper with rough surface), which is measured at the $1/e^2$ of its peak value with the CCD camera and the image processing system.

In practice, the output angle will increase slightly (less than 1°) with microbending, i.e., without specially wrapping, but if the fiber is wrapped into a circle, the difference of the angle will be up to 2° .

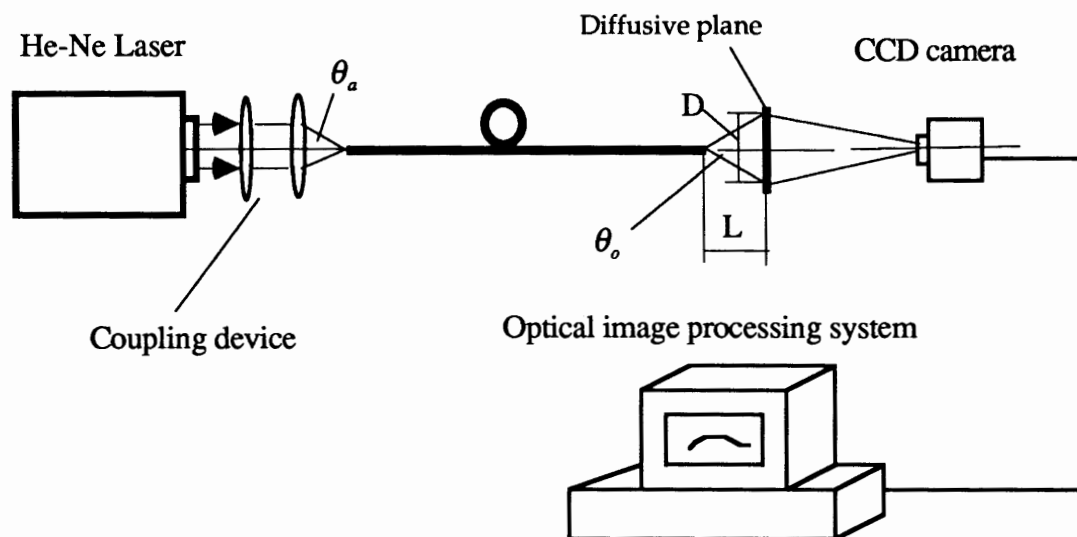


Figure 11. Experimental setup for convergence angle measurement.

EFFECT OF SCATTERING MATERIAL ON THE LIGHT DISTRIBUTION

The purpose of this experiment is to measure the effect of the scattering material (Al_2O_3 powder) on the light distribution at the tip. The irradiance distribution on the tip without powder and with powder is measured respectively. The experimental setup is shown in Figure 12. The tip is attached to a diffusive plane which is made of a piece of glass (0.1 mm thick) coated with UV epoxy (LITETAK 376, Loctite Co., Newington, CT0611) mixed with Al_2O_3 powder (the weight ratio of UV epoxy to Al_2O_3 powder is 10 to 3). The thickness is about 0.05 mm.

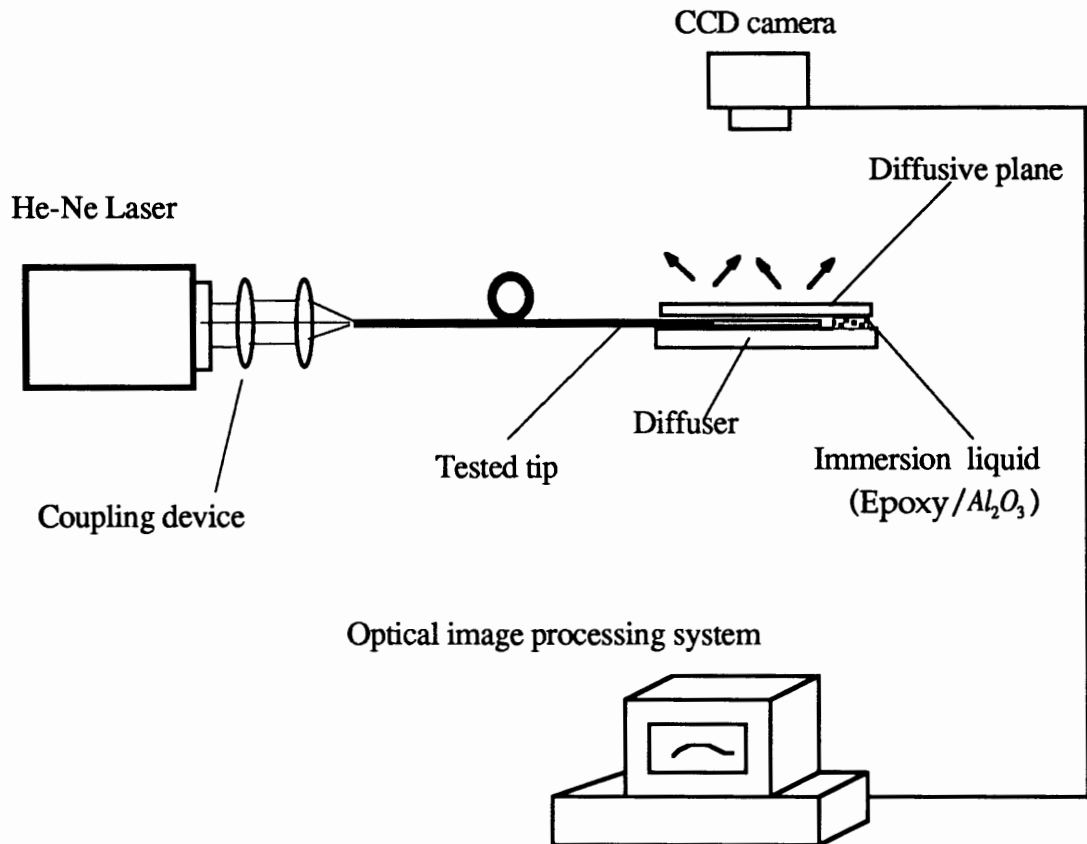


Figure 12. Experimental setup for measuring the effect of scattering material on the light distribution.

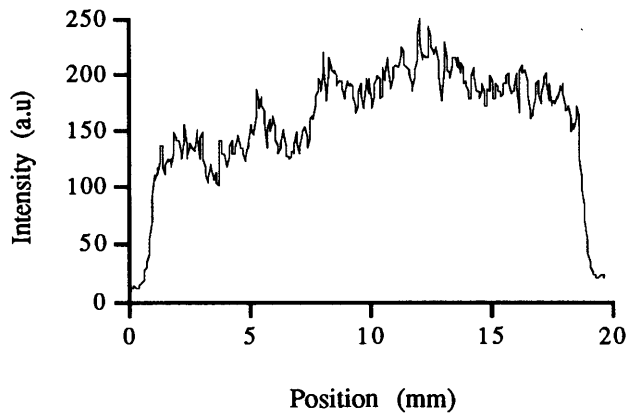
For the case without powder, since the small air bubbles in optical epoxy (EPO-TEK® 301-2) are very difficult to remove, we use an immersion liquid (R.P. CARGILLE LABORATORIES, INC., Cedar Grove, NJ 07009), whose refractive index is close to that of the optical epoxy, 1.57 at 633 nm, instead of the epoxy in this study. The large viscosity and surface tension of the immersion liquid permit us to directly drop the liquid on a glass diffuser and then the fiber could be inserted from above without the liquid leaking through the diffuser. The resulting pattern is intercepted with the diffusive plane and then captured by the CCD camera and image processing system whose output represents the light distribution on the tip surface since the diffusive plane is a reasonable good diffusing surface.

For the case with powder, the procedure is similar to that without powder, but the immersion liquid is replaced with the epoxy/powder mixture with two different concentrations.

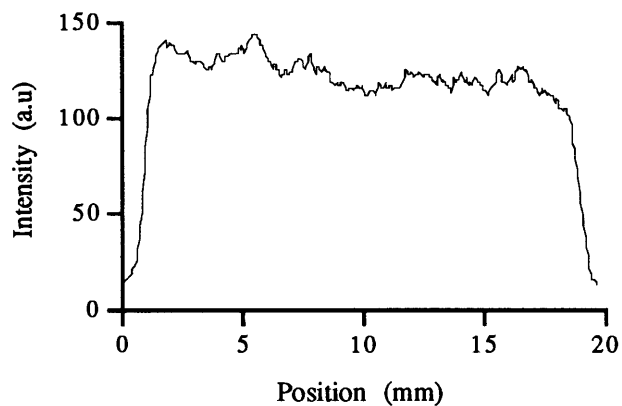
Figure 13 shows the measured irradiance for one fiber tip without powder and with powder.

EFFECT OF LIGHT COUPLING ON THE LIGHT DISTRIBUTION

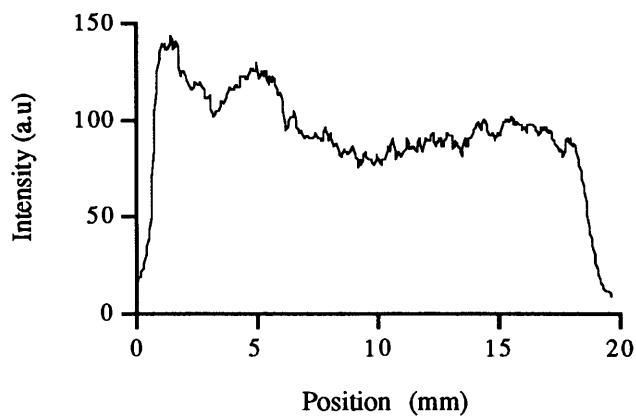
Since the tip is made on the basis of a known convergence angle of input beam, the light distribution will be changed with different convergence angles. An arrangement for measuring the irradiance distribution for one fiber tip with different convergence angles is shown in Figure 14.



(a)



(b)



(c)

Figure 13. Measured irradiance at one tip: (a) without powder; (b) powder concentration = 285 mg/ml; (c) powder concentration = 570 mg/ml. Fiber tip specifications: bi-tapered fiber length $L_t = 20$ mm, convergence angle of input beam $\theta = 5^\circ$.

The tip is inserted into water. The radial distance from the fiber axis to the surface of water is ~ 1.75 mm. The CCD camera is focused on the surface of water to capture the resulting irradiance pattern of laser energy. The results are shown in Figure 15. The measurement demonstrates that the convergence angle affects the irradiance distribution quite significantly.

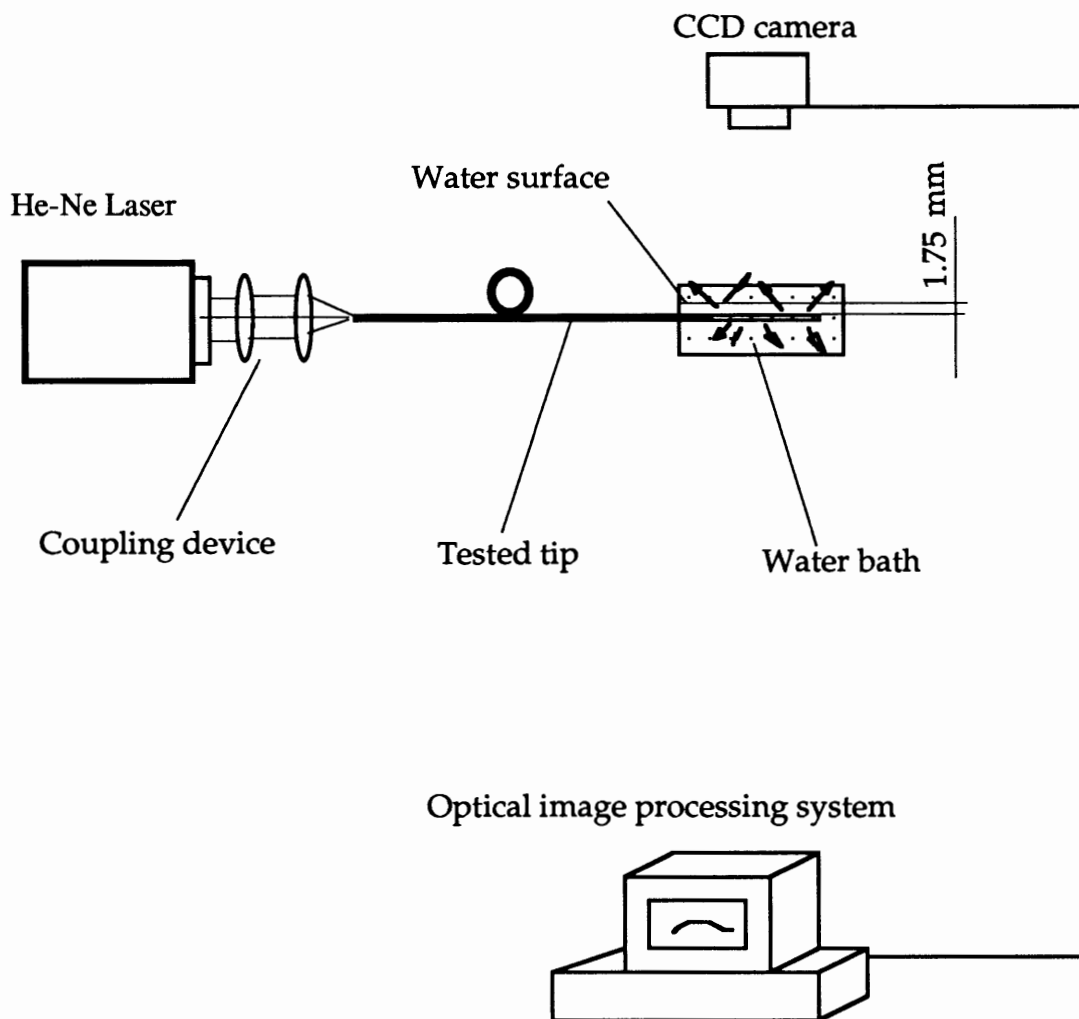
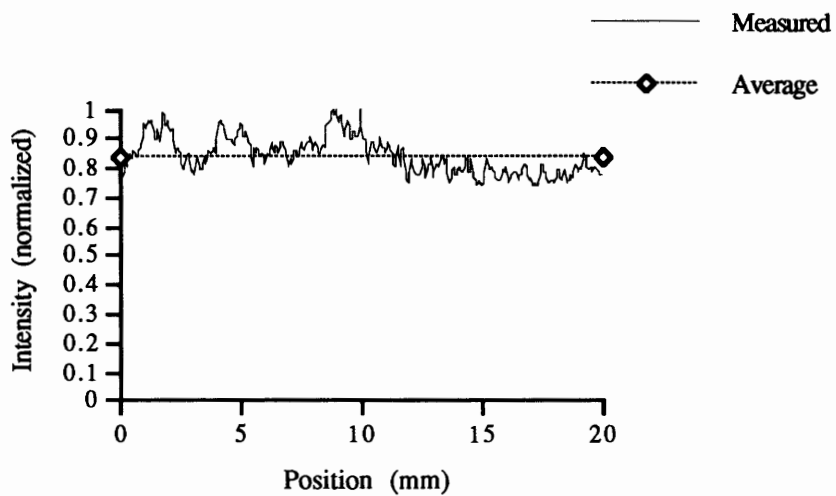
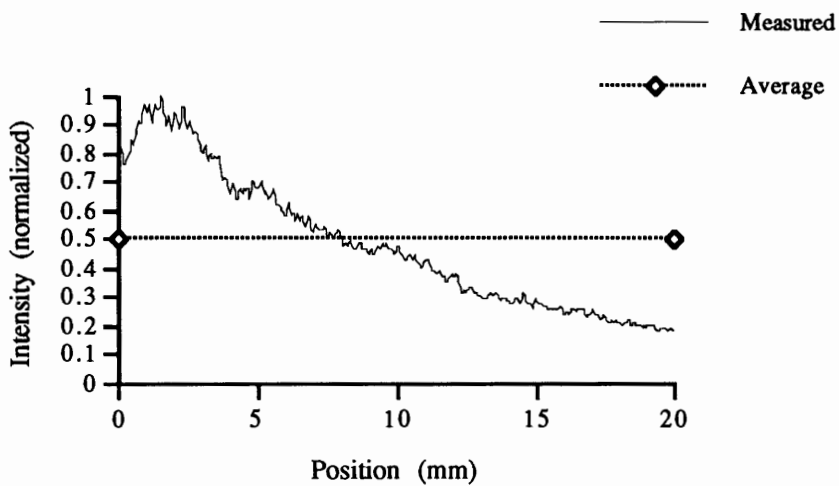


Figure 14. Arrangement for measuring the effect of light coupling on the light distribution.



(a)



(b)

Figure 15. Measured irradiance at a distance of 1.75 mm from the fiber axis for one fiber at two different convergence angles θ , normalized to the maximum value, for (a) $\theta = 5^\circ$; (b) $\theta = 8^\circ$. Fiber tip specifications: bi-tapered fiber length $L_t = 20$ mm, powder concentration = 285 mg/ml.

REPRODUCIBILITY OF THE FABRICATION TECHNIQUE

Four tips fabricated with the same fabrication technique are tested. Measurement apparatus for the reproducibility of the tip is shown in Figure 16. The procedure is to measure the irradiance distribution with the setup shown in Figure 16, and then to measure the total output power with an integrating sphere, a device used in conjunction with the radiometer to measure total optical power output from a diffuse source. The convergence angle of input beam in this experiment is $\sim 5^\circ$. The irradiance distributions of each tip are measured on three "sides" with respect to rotation. The deviation of the irradiance distributions is consistently under 5% for all four tips. The error bars are drawn representing standard deviation of the mean of the four average distributions of each individual illuminator tip. Results from the irradiance distribution measurements of four tips fabricated with the same fabrication technique are shown in Figure 17.

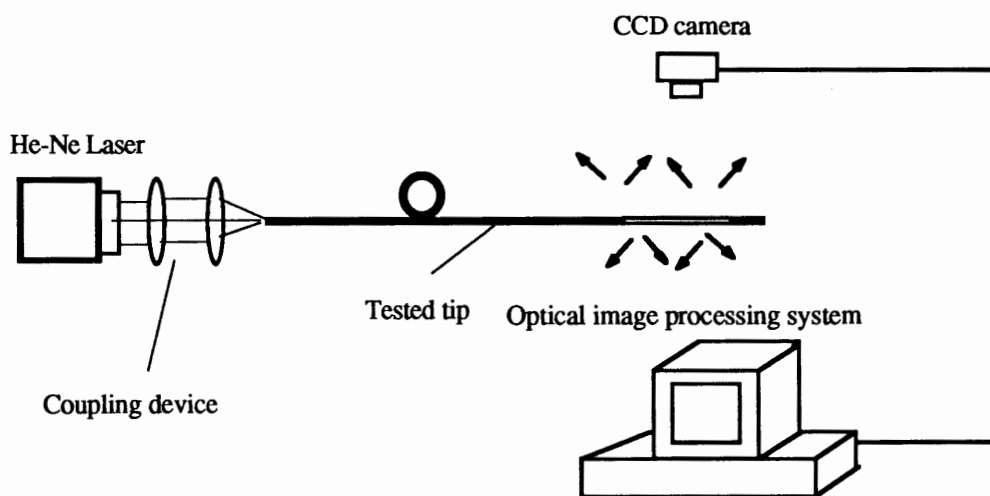


Figure 16. Measurement apparatus for the reproducibility of the tips.

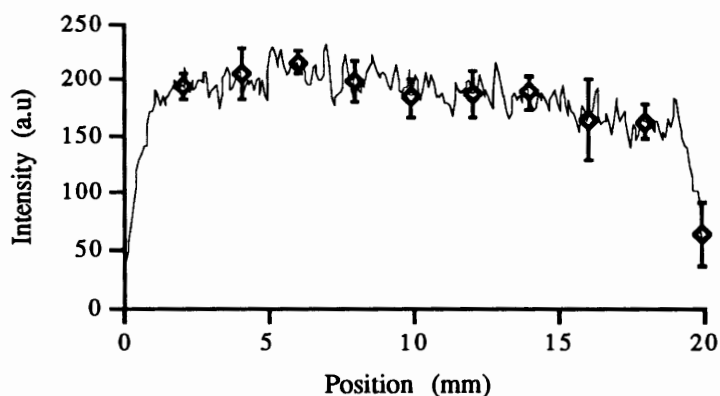


Figure 17. Measured irradiance showing the reproducibility of the fabrication technique. Fiber tip specifications: $L_t \sim 20$ mm, $\theta = 5^\circ$, powder concentration = 285 mg/ml.

RESULTS FOR THE DEVICE TO ILLUMINATE AN ANGIOPLASTY BALLOON

The assembly used for the device to illuminate an angioplasty balloon is shown in Figure 18. A Ti:Sapphire Ring Laser System with a doubling crystal (Model 899-01 Dye Ring Laser, COHERENT Laser Group, Palo Alto, CA 94303) pumped by an argon ion laser is used to generate the wavelength ($\lambda = 365$ nm) in this study. Since the performance of the illuminator tips is similar, we have chosen one of them to illuminate the angioplasty balloon in an experimental photochemotherapeutic treatment of swine intimal hyperplasia. The irradiance distributions are measured at four positions along the tip length and on four "sides" with respect to rotation (cf. Figure 18.)

The irradiance on the surface of an angioplasty balloon is intercepted with an isotropic fiber optic detector connected to a power meter (Model 351B, UDT Instruments, Orlando, FL32826), whose output represents a measure of the power level around the nearfield of the balloon. The irradiance distribution can

be determined by measuring the power level at a series of points along the balloon. The fiber scattering probe is made of 400 μm core fused silica fiber with a 0.5 mm diameter scattering probe and possesses an approximately isotropic response. The scattering material of the probe is UV epoxy/ Al_2O_3 powder mixture. The convergence angle of the input beam in this experiment is $\sim 5^\circ 9'$. The result is shown in Table II.

The light extraction efficiency of the device is $\sim 70\%$, considered with respect to the total optical power exiting the flat-cleaved fiber in comparison with that exiting the illuminator tip. During the measurement, the total optical power is measured with an integrating sphere. The transmission of the balloon material is $\sim 90\%$.

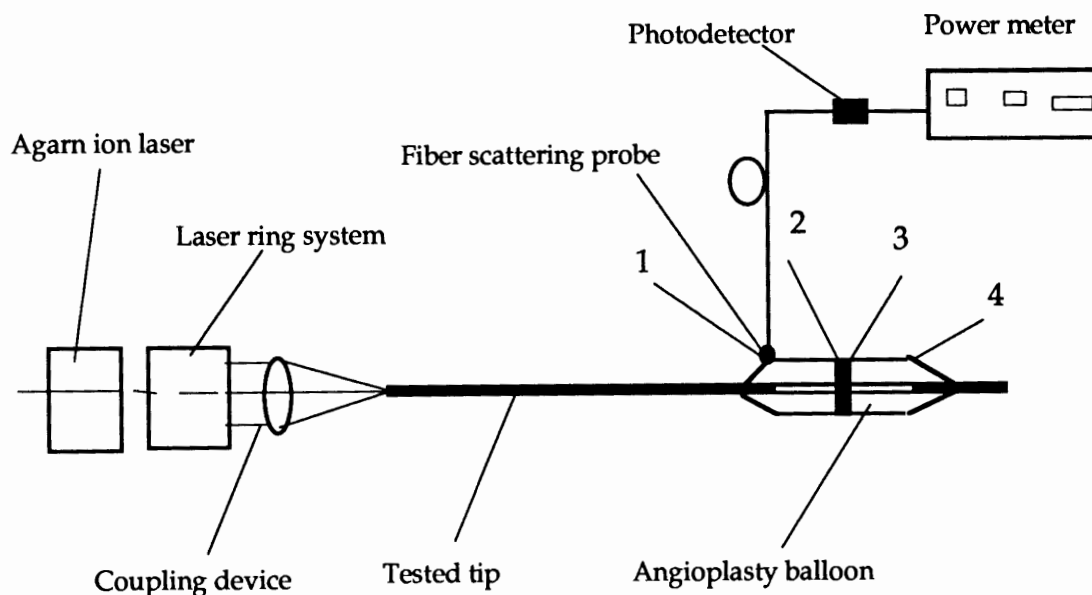


Figure 18. Assembly for the device to illuminate an angioplasty balloon.

TABLE II

MEASURED OPTICAL POWER ALONG AN ANGIOPLASTY BALLOON

Position No. Measured data(a.u)	1	2	3	4
Measurement No.				
1	1.90	2.00	1.69	1.72
2	1.95	1.90	1.63	1.58
3	1.68	1.72	1.62	1.60
4	1.70	1.58	1.61	1.54
Min. = 1.54, Average = 1.714, Max. = 2.00, δ = 0.145, Uniformity \pm 15%				

Fiber tip specifications: bi-tapered tip length $L_t \sim 20$ mm, $\theta = 5^\circ 9'$, powder concentration = 285 mg/ml.

CHAPTER VI

DISCUSSION

The light distribution of the illuminator tip is determined by the geometry of the tip, the convergence angle of input beam, the refractive indices of the core and the scattering layer, and the scattering powder concentration. Good uniformity can be obtained by optimizing these parameters. The fabrication technique used in this study is to modify the geometry of the tip on the basis of a given coupling condition. A more controllable situation would be the use of a low NA fiber (NA ~ 0.11) and a launch condition close to that NA. The disadvantage of our approach is that if the coupling condition in treatment changes, the light distribution will be changed significantly, for example, the uniformity varies from $< \pm 13\%$ of the average value at $\theta = 5^\circ$ to $\pm 42\%$ of that at $\theta = 8^\circ$ (see Figure 15.). However, in practice, the light distribution does not alter significantly as the convergence angle is changed within the range $\theta = 5^\circ \sim 6.5^\circ$. Optimization of the fiber tip for higher NA launch conditions is possible by increasing the taper angle. However, this way may cause the fiber structure to be more brittle, since more of the fiber core is etched away. Therefore, the smaller the taper angle α is, the more safety there is against fracture.

The light is coupled out of the fiber structure due to the different indices of refraction of the core and the scattering layer. The measurements in the section on Effect of Scattering Material on the Light Distribution (Chapter V) show that the scattering powder is necessary for improving the uniformity due to the

scattering function of the powder. Powder with higher refractive index will probably make the light scattering more efficient than powder with relatively lower refractive index⁶. We can not offer a rigorous explanation of the effects of higher powder concentration on the light distribution, but intuitive reasoning suggests that the scattering effect of the scattering layer may decrease [cf. Figure 13(a) – 13(c)]. The uniformity of illumination changes with increasing the powder concentration. At high concentrations, many of the particle boundaries are shared, or separated by distances much less than the wavelength, and contribute less to the scattering, i.e., saturation may occur at higher concentrations. This reflects the fact that, at high concentration, all light that enters the scattering layer is immediately scattered.

In the present work, we have introduced what is to our knowledge the first use of the new device configuration where the tip is etched into a modified conical shape, and the distal end face is polished and then coated with an optically opaque epoxy to achieve a uniform cylindrical pattern of laser energy with the uniformity $< \pm 15\%$ of the average value. The measurements demonstrate that the fabrication technique is suitable for producing an optical fiber diffusing tip with a uniform cylindrical irradiance pattern of laser energy and good reproducibility. However, in practice the illuminator tip can not be held in the center of the balloon due to the eccentricity of the balloon itself, and an eccentric distribution has resulted (see Table II). On the other hand, since the optical epoxy/ Al_2O_3 mixture is not flexible, the tip may be easily broken when it is bent close to 50° . Therefore, this diffusing tip in its current configuration will not be suitable for all vascular applications, specially where vascular anatomy involves vessel angulation $< 50^\circ$, for example, it is not suitable to be used with

hockey stick catheter (cf. Figure 19), but this problem may be solved with more flexible coating material and fiber than that used in this study.

Simple modifications in fabrication technique can alter the illuminator tip characteristics to suit different applications. We therefore expect this fabrication technique to be most useful for the design and fabrication of optical fiber diffusing devices for PDT with geometries, scattering materials, various types of fibers, etc., other than the present.

In this study, we have developed a computational model for calculating the light distribution along the bare core surface of an optical fiber tip and experimentally verified it. Good agreement is obtained between the calculation and experiment (cf. Appendix A). Although the model is very simple, it is suitable for simulating the light distribution along the bare core surface of an optical fiber tip and very useful for the design and fabrication of the diffusing tip.

The illuminator tip fulfills all of the design requirements that were set. The optimization of design and fabrication through mathematical modeling and improvement of the fabrication technique is currently in progress.

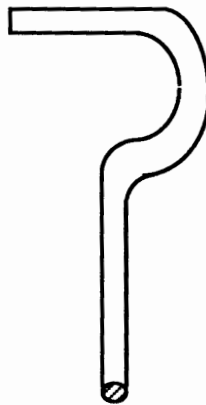


Figure 19. Schematic diagram of Hockey Stick Catheter.

CHAPTER VII

CONCLUSION

This study has yielded several important results: 1) The illuminator tip fulfills all of the design requirements of miniature size and uniformity of illumination. 2) An illuminator tip can be reliably made to obtain reproducible cylindrical dispersion of laser energy for ultraviolet light delivery in PDT using the fabrication technique we have developed. 3) The tip is reasonably durable, convenient, and inexpensive. 4) This device has been shown to uniformly (+/- 15%) illuminate angioplasty balloons, 20 mm in length, that are used in an experimental photochemotherapeutic treatment of swine intimal hyperplasia. 5) Our experiments show that diffusing tips of < 400 micron diameter can be reliably constructed for this and other interstitial applications. Modeling results indicate that this design is scalable to smaller diameters and thus small illuminators for PDT can also be fabricated in this way. 6) The basic computational model is suitable for simulating the light distribution on the bare core surface of an optical fiber tip and is also useful for the design and fabrication of the diffusing tip.

REFERENCES

1. Ralph de la Torre, and Kenton W. Gregory, "Cavitation Bubbles and Acoustic Transients May Produce Dissections During Laser Angioplasty," JACC Vol. 19, No. 3, March 1, 1992:48A.
2. Kenton W. Gregory, Joanne M. Wimberly, Peter C. Block, and R. Rox Anderson, "Inhibition of Smooth Muscle Cell Hyperproliferation by 8-methoxy Psoralen Activated by Ultraviolet Light," JACC Vol. 19, No. 3, March 1, 1992:169A.
3. Keith L. March, Brian L. Patton, Robert L. Wilensky, and David R. Hathaway, "8-Methoxypsoralen and Longwave Ultraviolet Irradiation Are a Novel Antiproliferative Combination for Vascular Smooth Muscle," Circulation, Vol. 87, No. 1, Jan. 1993.
4. Balchum OJ, Diron DR, and Huth GC, "Photoradiation therapy of endobronchial lung cancers employing the photodynamic action of hematoporphyrin derivative," Lasers in Surgery and Medicine, Vol. 4, pp. 13-30, 1984.
5. Mcphee MS, Thorndyke CW, Thomas G, Tulip J, Chapman D, and Lakey WH, "Interstitial applications of laser irradiation in hematoporphyrin derivative-photosensitized Dunning R3327 prostate cancers," Lasers in Surgery and Medicine, Vol. 4, pp. 93-98, 1984.
6. Lnnart Hasselgren, Sheila Galt, and Sverker Hard, "Diffusive optical fiber ends for photodynamic therapy: manufacture and analysis," Applied Optics, Vol. 29, No. 30, pp. 4481-4488, 1990.
7. M. Arnfield, S. Gonzalez, P. Lea, J. Tulip, and M. Mcphee, "Cylindrical irradiator fiber tip for photodynamic therapy," Laser in Surgery and Medicine, Vol. 6, pp. 150-154, 1986.
8. James T. Allardice, Adrian C. Rowland, Norman S. Williams, and C. Paul Swain, "A new light delivery system for the treatment of obstructing gastrointestinal cancers by photodynamic therapy," Gastrointestinal Endoscopy, Vol. 35, No. 6, pp. 548-551, 1989.

9. P. Lenz, "Light distributor for endoscopic photochemotherapy of tumors," *Applied Optics*, Vol. 26, No. 20, pp. 4452-4456, 1987.
10. Hugh L. Narciso, David V. Spain, and Daniel R. Doiron, "Third generation cylindrical diffusers for medical use", *SPIE Proceedings* Vol. 1893, 1893-28, 1993.
11. Buonaccorsi G. A., Burke T., McRobert A. J., Hill P.D., Essenpreis M., and Mills T. N., "A cylindrical distributing optical fiber tip for uniform illumination of hollow organs during laser therapy", *SPIE Proceedings* Vol. 1893, 1893-29, 1993.
12. N. S. Kapany, Fiber Optics, Academic, New York, 1967.
13. Max Born and Emil Wolf, Principles of Optics, pp. 45, Pergamo Press, 1970.
14. E. hecht and A. Zajak, Optics, Addison-wesly, Reading, MH1979.
- 15 W. Siegmand, "Fiber Optics" in Handbook of Optics, W. Driscoll and W. Vaughan. Eds, McGram-Hill, New York, 1978.
16. N. S. Kapany and D. F. Capellaro, "Fiber Optics. VII. Image Transfer from Lambertion Emitters", *J. Opt. Soc. Am.*, Vol. 51, No. 1, pp. 23-34, 1961.
17. D. Gloge, "Optical Power Flow in Multimode Fibers", *The Bell System Technical Journal*, Vol. 51, No. 8, pp.1767-1783, 1972.
18. Allan W. Snyder and D. J. Mitchell, "Leak rays on circular optical fibers", *J. Opt. Soc. Am.*, Vol. 64, No. 5, pp. 599-607, 1974.
19. J. P. Grenn, "Optical theory of Gaussian beam transmission thorough a hollow circular dielectric waveguide", *Applied Optics*, Vol. 21, No. 24, pp. 4533-4541, 1982.
20. Jacques Dugas, Michel Sotom, Louis Martin, and Jean-Michel Cariou, "Accurate characterization of the transitivity of large-diameter multimode optical fibers", *Applied Optics*, Vol. 26, No. 19, pp. 4198-4208, 1987.
21. Bertram S. Frost and Philip M. Gourlay, "Geometrical optical treatment of circular lightguides: general wall material", *Applied Optics*, Vol. 26, No. 23, pp. 5112-5117, 1987.

22. Alvaro A. P. Boechat, Daoning Su, D. R. Hall, and J.D.C. Jones, "Bend loss in large core multimode optical fiber beam delivery systems", *Applied Optics*, Vol. 30, No. 3, pp. 321-327, 1991.
23. C. T. Chang and D. C. Auth, "Radiation Characteristics of Tapered Cylindrical Optical Fiber", *J. Opt. Soc. Am.*, Vol. 68, No. 9, pp. 1191-1196, 1978.
24. H. Fujii, T. Asakura, T. Matsumoto, and T. Ohura, "Output power distribution of a large core optical fiber", *IEEE J. Lightwave Technol.* LT-2, pp. 1057-1062, 1984.
25. Martin R. Prince, Glenn M. LaMuraglia, Christine E. Seidlitz, Scott A. Prahl, Christos A. Athanassoulis, and Reginald Birngruber, "Ball-Tippered Fibers for Laser Angioplasty with the Pulsed-Dye Laser", *IEEE J. Quantum Electronics*, Vol. 26, No. 12, pp. 2297-2303, 1990.
26. Rudolf M. Verdaasdonk and Cornelius Borst, "Ray tracing of optically modified fiber tips. 1: Spherical probes", *Applied Optics*, Vol. 30, No. 16, pp. 2159-2171, 1991.
27. Rudolf M. Verdaasdonk and Cornelius Borst, "Ray tracing of optically modified fiber tips. 2: Laser scalpels", *Applied Optics*, Vol. 30, No. 16, pp. 2172-2177, 1991.
28. Daoning Su, Alvaro A. P. Boechat, and Julian D. C. Jones, "Beam delivery by large-core fibers: effect of launching conditions on near-field output profile", *Applied Optics*, Vol. 31, No. 27, pp. 5816-5820, 1992.
29. Ivan Melnik, Rudolf Stiner, Raimund Hibst, Manfred Fischer, and Gabriela Flemming, "Aspherically modified fiber tips have better focusing effect", *SPIE Proceedings Vol. 1878*, 1878-32, 1993.
30. Ivan Melnik, Manfred Fischer, Gabriela Flemming, and Raimund Hibst, "Forming of laser beams by optical fibers with beveled tips", *SPIE Proceedings Vol. 1893*, 1893-27, 1993.
31. Anpei Pan and Dipak Biswas, "Light distribution from optical fiber diffusing tips", *SPIE Proceedings Vol. 1893*, 1893-35, 1993.
32. R. Worthington, "Acceptance-angle measurement of multimode fibers: a comparison of techniques," *Applied Optics*, Vol. 21, No. 19, pp. 3515-3519, 1982.

33. Aharon Sagi, Avraham Shitzer, Abraham Katzir, and Solange Akselrod, "Heating of biological tissue by laser irradiation: theoretical model", *Optical Engineering*, Vol. 31, No. 7, pp. 1417-1423, 1992.
34. Joseph T. Verdeyen, Laser Electronics, Prentice Hall, Inc., New Jersey, 1989.

APPENDIX A

CALCULATION OF LIGHT DISTRIBUTION ON THE BARE CORE SURFACE OF THE FIBER TIP

APPENDIX A

CALCULATION OF LIGHT DISTRIBUTION ON THE BARE CORE SURFACE
OF THE FIBER TIP

BASIC COMPUTATIONAL MODEL

It has long been widely accepted that geometric optics, i.e., ray tracing using Snell's laws and Fresnel's coefficients, provides a good approximation of the light-acceptance and transmission properties of optical fibers when the ratio of fiber radius to wavelength is large, and most commercial laser beams have a Gaussian-shaped profile³³, given by:

$$I(r) = I_0 \cdot \exp\left(-2 \cdot \frac{r^2}{w^2}\right) \quad (\text{A1})$$

where I_0 is the intensity on axis, I is the intensity at a radial distance r from the axis and w is a measure of the beam radius. For this definition, the beam is defined in terms of its total power (or energy) and its diameter as measured at the $1/e^2$ of its peak value ($I/I_0 = 0.14$) so the area defined contains 86.5% of the total power in the beam.

On the basis of the geometric optics and Gaussian approximation, we treat the laser beam as a bundle of simple rays to be launched into the fiber with Gaussian angular distribution, starting on the center of the input end surface of the fiber as a point source. The fiber tip with the cladding removed is assumed

to be immersed in an index matching fluid, whose refractive index is very slightly higher than that of the core (in practice the difference can be made less than 1%). For the sake of simplicity, the following additional assumptions are made:

1. The fiber tip is cylindrical, straight and of dimensions large compared with the radiation wavelength.
2. The laser radiation has a uniform transverse illumination across the core and at each point has an angular intensity distribution which is symmetrical about the Z (i.e., fiber axis).
3. There are no second reflections between the core and the index matching fluid.

Figure A1 shows the basic computational model.

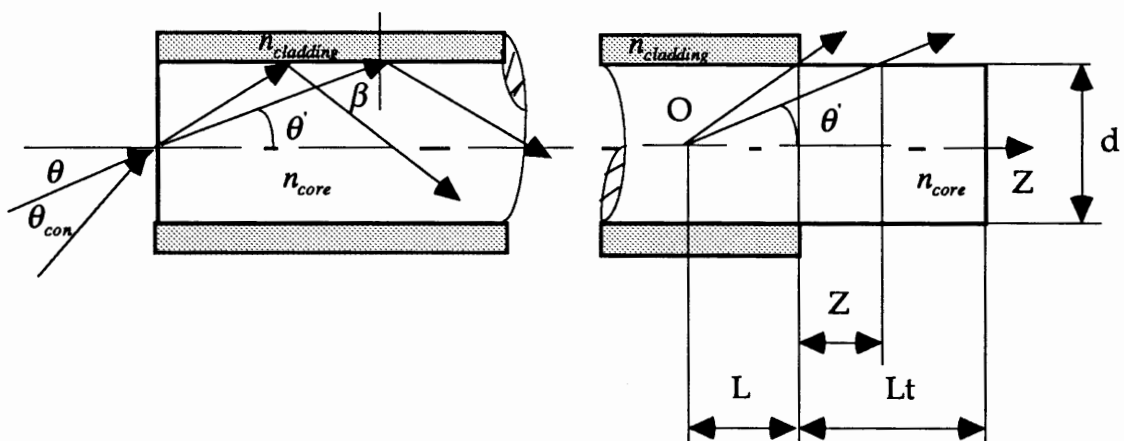


Figure A1. Basic computational model

The Z axis is assumed to be along the fiber axis, and also forms the symmetry axis of the fundamental mode laser beam. The fundamental mode laser beam can be approximated by an arbitrary Gaussian input

$$I_{in}(\theta) = I_o \cdot \exp\left(-2 \cdot \frac{\theta^2}{\theta_{con.}^2}\right) \quad (A2)$$

where θ is the coupling angle, $\theta_{con.}$ is the convergence angle of the input beam. The derivation of Equation (A2) is shown in Appendix B.

An arbitrary ray at an angle θ is refracted at the entrance end to an angle θ' to the Z axis and strikes the wall of the core at an angle $\beta [=(\pi/2)-\theta']$. So long as the angle β is equal to or greater than the critical angle [$\arcsin(n_{cladding} / n_{core})$], this wave will be totally reflected and strike the other side of the core at the same angle. Thus, this ray will be trapped inside the core, undergo multiple total internal reflections, and emerge only at the other end of the fiber. For a claimed straight cylindrical fiber, the emergent angle of the meridional rays is the same as the entrance angle. However, for a fiber tip with the cladding removed, the rays will be directly transmitted to the index matching fluid.

As shown in Figure A1, rays entering at smaller angles take more direct paths than larger ones. Since all rays will travel at the same speed, some rays, those with the shortest path length, or those accepted normal to the fiber face, will reach the other end of the fiber first. Those accepted at slightly lower angles to the normal will arrive next, etc., until those introduced at a convergence angle $\theta_{con.}$ (equal to or less than the fiber numerical aperture NA) will exit end of the

fiber last. Thus, we assume those rays are emitted from a point source O (see Figure A1).

According to the cosine law of illumination and the inverse square law¹³, The irradiance distribution on the core surface is given by:

$$E(\theta, \beta, Z) = \frac{I_o}{(L+Z)^2 + d^2} \cdot \exp\left(-2 \cdot \frac{\theta^2}{\theta_{con.}^2}\right) \cdot \cos\beta \quad (A3)$$

where $L = \frac{d \cdot n_{core}}{2 \cdot NA}$, $\theta = \arctan\left[\frac{d}{2 \cdot (L+Z)}\right] \cdot n_{core}$, β is the angle which the propagating direction of the ray makes with the normal to the surface element, i.e., the incident angle on the unclad core surface. In our case, since the irradiance is directly measured on a diffusive plane which is a reasonable good diffusing plane or with an isotropic probe, we assume each ray is normal to the control surface of detector, therefore, $\cos\beta = 1$, Z is the coordinate along the fiber axis.

Using Eq. (A3), we can simulate the optical behavior of the laser beam propagating along the core surface of an unclad multimode optical fiber with various geometries and the input beam.

NUMERICAL AND EXPERIMENTAL RESULTS

In this study the light distribution along the bare core surface of fiber tips with different geometries, i.e., cylindrical and modified geometries, is measured and calculated respectively.

The experimental setup for the cylindrical geometry is shown in Figure A2. The light distribution along the bare core surface is measured with the same method as that described in the section on Effect of scattering Material on Light Distribution (Chapter V), but the index matching fluid (R.P. CARGILLE LABORATORIES, INC., Cedar Grove, NJ 07009) is used in this experiment. For easy of adjusting convergence angle, we use fiber-fiber coupling. An arc lamp source (ORIEL, Co., Stratford, CT 06497) is used as the light source. The beam profile is similar to that of Gaussian beam.

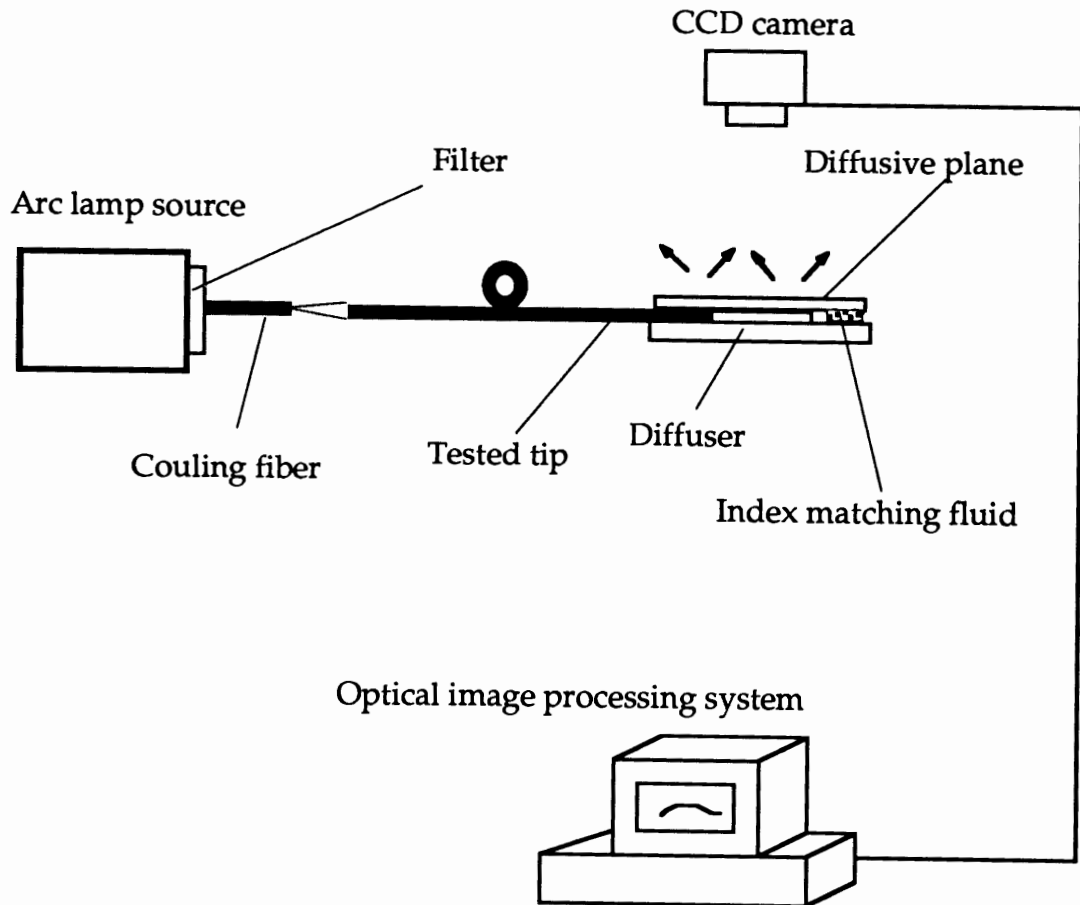


Figure A2. Experimental setup for measuring the light distribution on the bare core surface of a fiber tip with cylindrical geometry.

Both distal faces of the coupling fiber, a silica optical fiber with 400 μm core diameter (Polymicro Technologies, Phonix, AZ), are wet-polished flat. The various convergence angles can be easily obtained through adjusting the distance between the two fibers. A filter ($\lambda = 404.7 \text{ nm}$) is used in this experiment.

In this study, we have chosen three groups of data with different convergence angles (cf. Figure A3 and Figure A5), and different core diameters (cf. Figure A3 and Figure A4) to calculate the light distribution along the bare core surface of the fiber tips.

Figures (A3 – A5) show the measured and calculated irradiances for different cases, normalized to the maximum value.

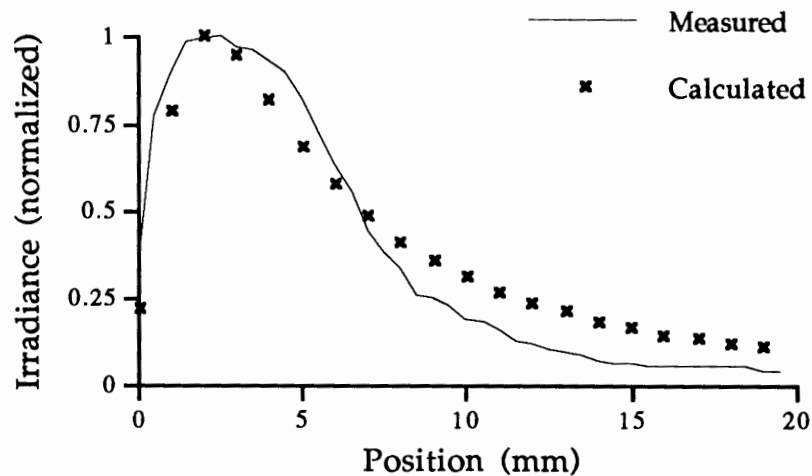


Figure A3. Case 1. Fiber tip specifications: $\text{NA} = 0.22$ radian, $\theta_{\text{con.}} = 0.16$ radian, $d = 699 \mu\text{m}$, $n_{\text{core}} = 1.47$, $L_t = 20 \text{ mm}$.

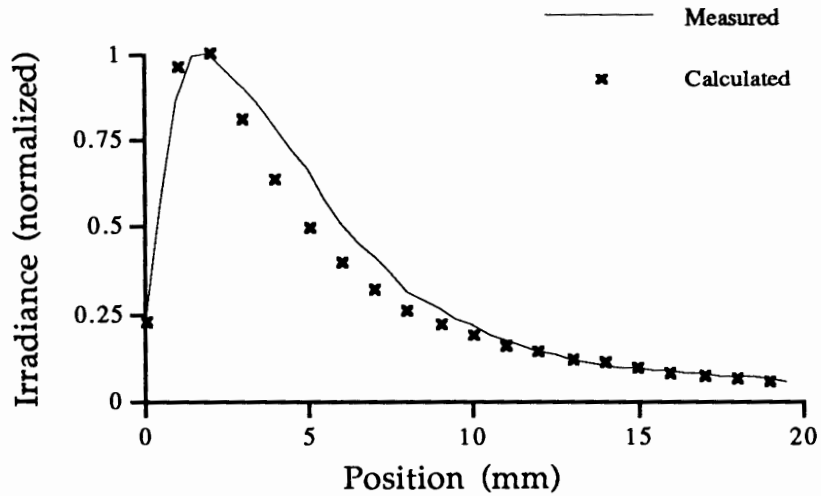


Figure A4. Case 2. Fiber tip specifications: NA = 0.22 radian, $\theta_{con.} = 0.16$ radian, $d = 469 \mu\text{m}$, $n_{core} = 1.47$, Lt = 20 mm.

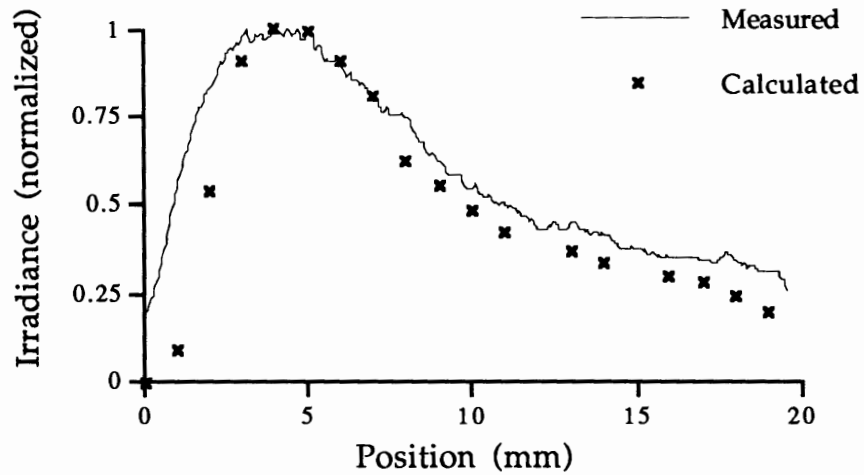


Figure A5. Case 3. Fiber tip specifications: NA = 0.22 radian, $\theta_{con.} = 0.085$ radian, $d = 469 \mu\text{m}$, $n_{core} = 1.47$, Lt = 20 mm.

The experimental setup for the modified geometry is shown in Figure A6. The irradiance on the modified bare core surface of the fiber tip is intercepted

with an isotropic fiber optic detector connected to a power meter (Model 351B, UDT Instruments, Orlando, FL32826), whose output represents a measure of the power level around the nearfield of the bare tip. The irradiance distribution can be determined by measuring the power level at a series of points along the surface. The fiber scattering probe is made of 400 μm core fused silica fiber with a 0.5 mm diameter scattering probe and possesses an approximately isotropic response. The scattering material of the probe is UV epoxy/ Al_2O_3 powder mixture. The probe is controlled by a translator (Line Tool Co., AllenTown, PA) with three dimensional position. The convergence angle of the input beam in this experiment is $\sim 5^\circ$.

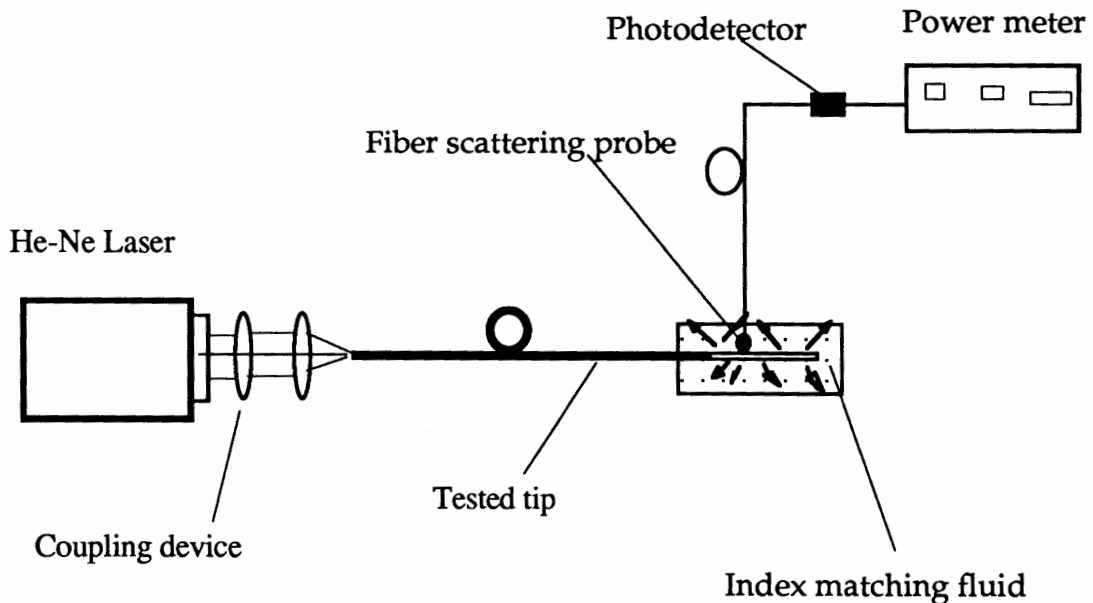


Figure A6. Experimental setup for measuring the light distribution on the bare core surface of a fiber tip with modified geometry.

It is very difficult to control the probe to be very close to the surface without touching it since the core is transparent and the diameter of the core is very small. The irradiance distribution is measured on three “sides” with respect to rotation. The error bars are drawn representing standard deviation of the mean of three measurements. The results are shown in Figure A7.

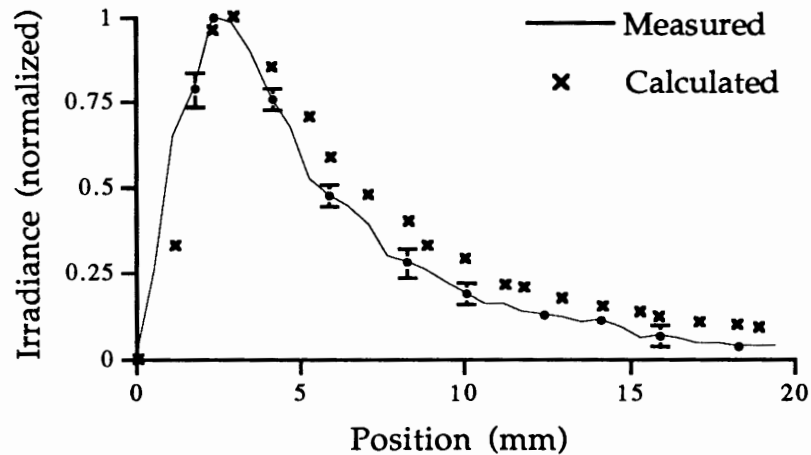


Figure A7. Measured and calculated irradiance, normalized to the maximum value, Fiber tip specifications: NA = 0.22 radian, $\theta_{con.} = 0.087$ radian, $d \sim$ (cf. Table I), $n_{core} = 1.46$, Lt = 20 mm.

The data (cf. Figure A3 – Figure A5, Figure A7) show that the computational model can be used to predict the light distribution on the bare core surface of a fiber tip. It is useful for fabrication of the diffusing tip, e.g., we can know whether the cladding is removed cleanly or not. The model can also be used to determine the covered position. In practice the irradiance peak position is ~ 3 mm from the beginning of the tip (cf. Table I) during the fabrication, which agrees to the calculated data.

APPENDIX B

DERIVATION OF Eq. (A2)

APPENDIX B

DERIVATION OF Eq. (A2)

The purpose of this appendix is to show how the Gaussian beam given as Eq. (A1) (a function of radial position) can be transferred into a function of angular position given as Eq. (A2). From Eq. (A1), the intensity of a Gaussian beam on the center of the input end is given by:

$$I(r, z) = I(0, z) \cdot \exp\left(-2 \cdot \frac{r^2}{w^2}\right) \quad (\text{B1})$$

where z is the fiber axis, r is the radial coordinate, w is the beam spot size at the $1/e^2$ points of the intensity profile (see Figure B1).

Accordingly, the classical relations³⁴ giving the parameters of the Gaussian beam can be written as

$$w(z) = w_0 \left[1 + \left(\frac{z}{kw_0^2} \right)^2 \right], \quad (\text{B2})$$

$$R(z) = z \left[1 + \left(\frac{kw_0^2}{z} \right)^2 \right], \quad (\text{B3})$$

where R is the radius of curvature of the Gaussian beam, k is the free space propagation constant $k = 2\pi / \lambda$. The beam contracts to minimum spot size w_0 at the beam waist.

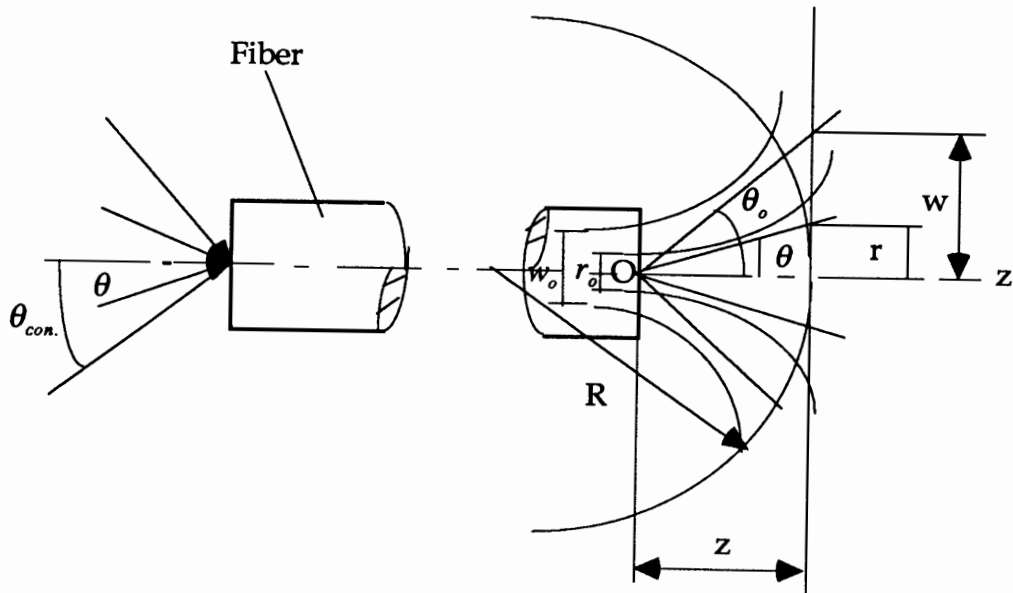


Figure B1. Main parameters of a Gaussian beam

Then, two basic assumptions about Gaussian beams will be used in the derivation:

1. Each ray path and its asymptote are assumed to be coincident.
2. The beam divergence as defined by the angle θ_0 (see Figure B1) is assumed to be very small so that their sines or tangents can be replaced by their arguments (i.e., $\sin \theta_0 \approx \tan \theta_0 \approx \theta_0$) for all rays with non-negligible intensity.

From assumption 1, Eqs. (B2), (B3) can be written

$$w = \frac{z}{kw_0} \quad (\text{B4})$$

$$R = z \quad (\text{B5})$$

That means the beam is composed of optical rays passing by the common point O (see Figure B1).

From assumption 2 , we obtain

$$\theta_o = \frac{w}{z} = \frac{1}{kw_o} \quad (\text{B6})$$

From Figure B1 and with the assumption 1, we obtain

$$\frac{\theta}{\theta_o} = \frac{r}{w} \quad (\text{B7})$$

Since, $\theta_o \approx \theta_{con.}$, the expression for $I(\theta)$ is

$$I(\theta) = I_o \cdot \exp\left(-2 \cdot \frac{\theta^2}{\theta_{con.}^2}\right) \quad (\text{B8})$$